Molecular and virological studies of viruses isolated from bats
（コウモリから単離されたウイルスのゲノムおよびウイルス性状に関する研究）

Kittiya Intaruck

Contents

List of Figures

List of Tables

Abbreviations

μm	Micrometer
ACE2	Angiotensin-converting enzyme 2
ACTB	β-actin
ANOVA	Analysis of Variance
ARV	Avian orthoreovirus
BHK-21	Baby hamster kidney-21
BIC	Bayesian information criterion
BLASTn	Basic local alignment search tool for nucleotide
bp	Base pairs
BrRV	Broome orthoreovirus
BRV	Baboon orthoreovirus
BW	Body weight
CCL2	Chemokine (C-C motif) ligand 2
CD3	Cluster of differentiation-3
COVID-19	Coranavirus disease 2019
CPE	Cytopathic effect
CXCL10	Chemokine (C-X-C motif) ligand 10
DDBJ	DNA data bank of Japan
DMEM	Dulbecco's Modified Eagle Medium
DNA	Deoxyribonucleic acid
dpi	Days post-inoculation
EIDs	Emerging infectious diseases
FAST	Fusion-associated small transmembrane

FBS	Fetal bovine serum
FFA	Focus forming assay
ffu/ml	Focus-forming units per milliliter
G	Gamma-distributed
GTR	General Time Reversible
H&E	Hematoxylin and Eosin
HEK293T	Human embryonic kidney 293T cell
HK/07	HK23629/07 strain
HK/09	HK46886/09 strain
HK/10	HK50842/10 strain
hpi	Hour post-infection
HTS	High-throughput sequencing
I	Invariant sites
Iba1	Ionized calcium binding adaptor molecule 1
IFA	Immunofluorescence assay
IFB	Indonesian fruit bat
IFN-β	Interferon-beta
IFN-γ	Interferon-gamma
IgG	Immunoglobulin G
IHC	Immunohistochemistry
IL-6	Interleukin-6
iTOL	Interactive Tree Of Life
KamV	Kampar virus
MAHLV	Mahlapitsi orthoreovirus

MB/07	Miyazaki-Bali/2007
MelV	Melaka virus
MEM	Minimum Essential Medium
MERS	Middle East respiratory syndrome
ML	Maximum-likelihood
mm	Millimeter
MOI	Multiplicity of infection
MPO	Anti-myeloperoxidase
MRV	Mammalian orthoreovirus
NA	Not available
NARV	Neoavian orthoreovirus
NBV	Nelson Bay orthoreovirus
NCBI	National Center for Biotechnology Information
nm	Nanometer
ORF	Open reading frame
ORV	Orthoreovirus
PBS	Phosphate buffer saline
pfu	Plaque-forming unit
PgORV	Paguyaman orthoreovirus
PRNT	Plaque reduction neutralization test
PRV	Piscine orthoreovirus
PuV	Pulau virus
qRT–PCR	Quantitative reverse transcription polymerase chain reaction
RdRp	RNA-dependent RNA polymerase

RNA	Ribonucleic acid
RRV	Reptilian orthoreovirus
RT-PCR	Reverse transcription polymerase chain reaction
Sarbecovirus	SARS betacoronavirus
SARS-CoV	Severe acute respiratory syndrome coronavirus
SARS-CoV-2	Severe acute respiratory syndrome coronavirus-2
SD	Standard deviation
SEA	Southeast Asia
sp.	Species
$TCID_{50}$	50% tissue culture infectious dose
TEM	Transmission electron microscope
TMPRSS2	Transmembrane protease serine 2
TNF	Tumor necrotic factor
TRV	Testudine orthoreovirus
UTR	Untranslated region
Vero T2	Vero E6-stably expressing TMPRSS2
Vero T2-AcACE2	Vero T2-expressing *Acerodon celebensis* ACE2
Vero T2-DmACE2	Vero T2-expressing *Dobsonia moluccensis* ACE2
Vero T2-hACE2	Vero T2-co-expressing human ACE2
VFL	Virus factory-like structure
w/v	Weight by volume
WHO	World Health Organization

Notes

Chapter I:

Intaruck K, Itakura Y, Kishimoto M, Chambaro HM, Setiyono A, Handharyani E, Uemura K, Harima H, Taniguchi S, Saijo M, Kimura T, Orba Y, Sawa H, Sasaki M. Isolation and characterization of an orthoreovirus from Indonesian fruit bats. ***Virology***. 575, 10-19, August 2022.

Chapter II:

Intaruck K, Tabata K, Itakura Y, Kawaguchi N, Kishimoto M, Setiyono A, Handharyani E, Harima H, Kimura T, Hall WW, Orba Y, Sawa H, Sasaki M. Characterization of a mammalian orthoreovirus isolated from the large flying fox, *Pteropus vampyrus* in Indonesia.

General introduction

Emerging infectious diseases (EIDs) pose a significant threat to global public health, economies, and biodiversity. The emergence and re-emergence of infectious diseases highlight the dynamic interactions between humans, animals, and the environment[1]. For outbreaks of emerging diseases, there are several contributing factors, such as increased human-animal interaction by urban sprawl, deforestation, and agricultural intensification. These circumstances disrupt the delicate balance in natural ecosystems and result in spillover events of viruses from wildlife to humans.

Historical outbreaks of divergent viruses, such as severe acute respiratory syndrome coronavirus (SARS-CoV), Middle East respiratory syndrome coronavirus (MERS-CoV), Nipah virus, and Ebola virus, have underscored the need for global health preparedness. In 2018, the World Health Organization (WHO) has termed "Disease X" to describe an unknown pathogen that could cause a future epidemic or pandemic[2]. The concept of Disease X emphasizes the importance of being prepared for unknown threats by representing the idea that the next major infectious disease outbreak could be caused by a pathogen currently unknown to cause human disease. It was introduced as a placeholder for planning and preparation, aiming to ensure that global health systems can respond effectively to unknown threats as they emerge.

The most concerning EIDs are those originating from zoonotic sources, particularly bats, which have been identified as reservoirs for several pathogenic viruses[3-5]. The emergence of bat-borne diseases in humans is a growing concern. As human populations continue to encroach on bat habitats, the risk of spillover events, in which a virus jumps from bats to humans, is likely to be increased[4-5].

One of the most well-known emergences of bat-borne viral diseases is a coronavirus responsible for the Coronavirus disease 2019 (COVID-19) pandemic, SARS-CoV-2. While the exact origins of the virus are still under investigation, evidence suggest that it may have been originated in bats before spilling over into humans, possibly through an intermediate animal host[6-8]. Research into the natural history of coronaviruses in bats has provided valuable insights into the emergence and transmission of SARS-CoV-2 and other SARS-CoV-2-related viruses.

It is crucial for understanding the dynamics of emerging infectious diseases and mitigating the risk of future outbreaks. Advance of technology and scientific knowledge, such as high-throughput sequencing (HTS) and metagenomic studies have accelerated the ability to identify novel viruses within bat populations. The metagenomic approach emerges as a

powerful tool, offering a glimpse into the unseen world of bat viruses. The core principle of a metagenomic approach lies in its ability to analyze the entirety of viral genetic material in samples, irrespective of whether the viral sequences are known or unknown. This unbiased technique allows researchers to cast a wide net, capturing not only known bat viruses but also novel ones that might have not been detected by conventional methods.

The metagenomic information are useful to understand the diversity and evolution of viruses in bats; however, those are insufficient to evaluate the virological characteristics, pathogenicity and zoonotic potential. Isolation of viruses from bats is a pivotal aspect to understand the virological properties and potential threat posed by bat-borne viruses but is one of the significant challenges in bat-borne virus research. Although numerous viral sequences were detected from bats, isolation of infectious viruses from bat samples was less successful[5].

In this dissertation, I focused on molecular and virological studies of bat-borne viruses by employing conventional methods, including virus isolation, electron microscopy, serological study, reverse transcription polymerase chain reaction (RT-PCR) technique, immunoassays and animal experiments, and advanced methods such as HTS. In the present studies, virus isolation was conducted from samples of fruit bats collected in Indonesia using an RT-PCR screening-based and cultured cell-based approaches, and the viruses belong to the genus *Orthoreovirus* were successfully isolated (Figure 1).

Among the viruses harbored by bats, the genus *Orthoreovirus* in the subfamily *Spinareovirinae*, the family *Reoviridae* are reported[9-34]. Orthoreovirus (ORV) is known to cause respiratory and gastrointestinal tract diseases in humans. There are 10 species belong to this genus, including Mamalian orthoreovirus (MRV), Avian orthoreovirus (ARV), Nelson Bay orthoreovirus (NBV), Baboon orthoreovirus (BRV), Reptilian orthoreovirus (RRV), Mahlapitsi orthoreovirus (MAHLV), Piscine orthoreovirus (PRV), Broome orthoreovirus (BrRV), Neoavian orthoreovirus (NARV), and Testudine orthoreovirus (TRV) (Figure 2). ORV is a non-enveloped, icosahedral shape consisting of ten linear double-stranded RNA segments with three large segments (L1–L3), three medium segments (M1–M3), and four small segments (S1–S4). ORV can be subdivided into fusogenic and non-fusogenic groups based on the ability to form multinucleated syncytial cells. Most species of ORV, except for MRV and PRV, are fusogenic and encode a fusion-associated small transmembrane (FAST) protein influencing syncytial formation.

To date, three species in the genus *Orthoreovirus* have been identified from bats; MRV,

NBV, and BrRV[9-34]. MRV was the first discovered species of reovirus, detected from a wide host range, including bats. Bat MRVs were reported in insectivorous bats in Europe, Canada, the United States of America (USA), China, Japan, and South Korea[10-13, 28-34], while NBV and BrRV were detected from fruit bats in the family *Pteropodidae*[9, 14, 17-22]. MRV typically causes coryza-like symptom and mild gastroenteritis in children[35-37]. Occasionally, MRV was a causative pathogen of encephalitis, meningitis, and hepatobiliary atresia in infants[37-40]. However, a zoonotic potential of MRV posed by domestic animals and wildlife, including bats is currently unclear and has to be elucidated. On the other hand, NBV is an emerging bat-borne disease that firstly emerged in humans in Malaysia in 2006[27]. NBV caused acute respiratory tract infection with influenza-like illness and human-to-human transmission have been reported[23-27]. Several NBV strains have been reported from fruit bats and respiratory tract infection patients in Southeast Asea (SEA) countries, especially Malaysia and Indonesia, indicating high prevalence of NBV in this region[17, 20-27]. This information emphasizes the importance of bat ORVs as a public health concern; however, a disease associated with BrRV has not yet been reported[16].

In chapter I of this dissertation, RT-PCR screening of ORV in wild fruit bats in Indonesia and viral isolation from RT-PCR positive samples were performed. The virus belonging to the NBV species was successfully isolated from fecal samples collected from Indonesian fruit bats (IFBs) and characterized its genome and virological properties as well as serosurveillance of NBV infections in IFB sera. In chapter II, throat swabs, lung and fecal samples of IFBs were inoculated onto various cell lines for virus isolation. MRV was recovered from cells inoculated with fecal samples of bats. After isolation of the MRV, phylogenetic analysis based on its full genome and virological examination by *in vitro* and *in vivo* experiments were performed.

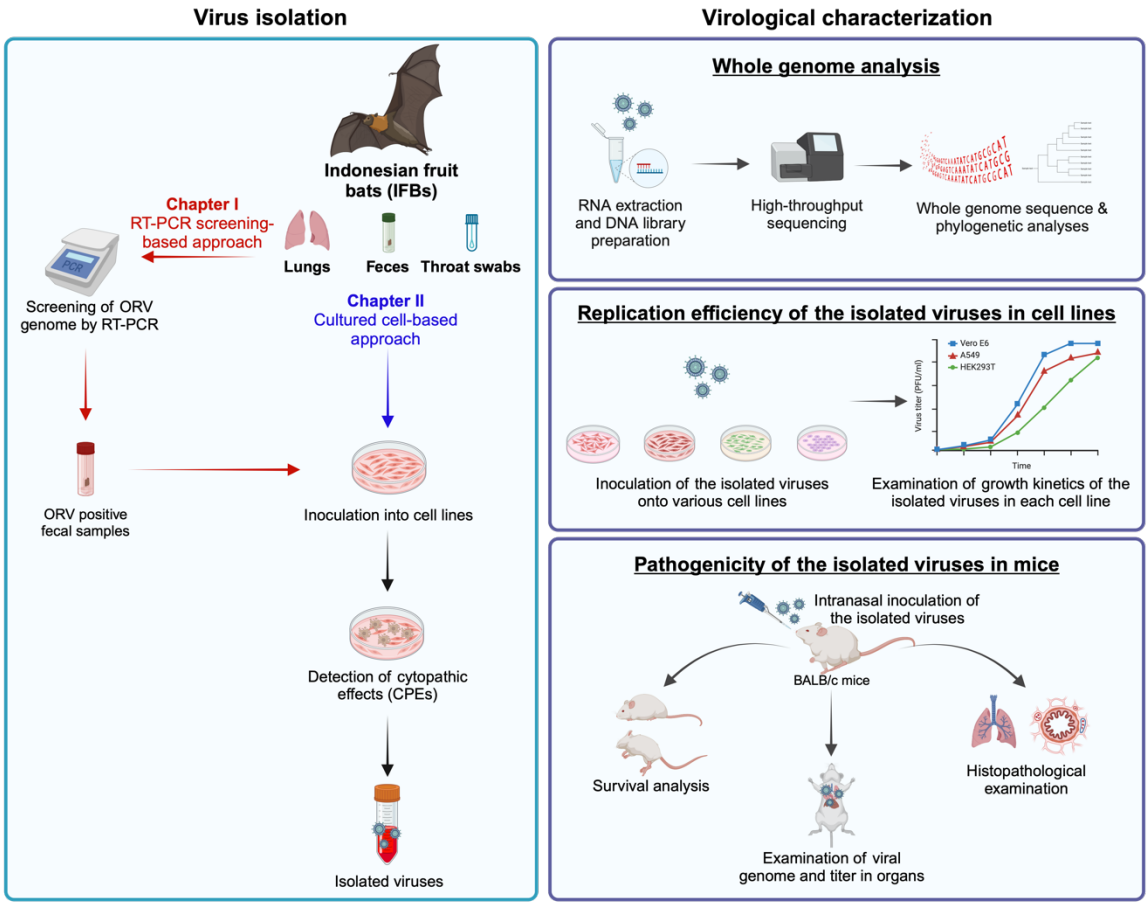

Figure 1. Schematic illustration of isolation and characterization of ORVs in this study.

The graphical scheme was created with BioRender.com.

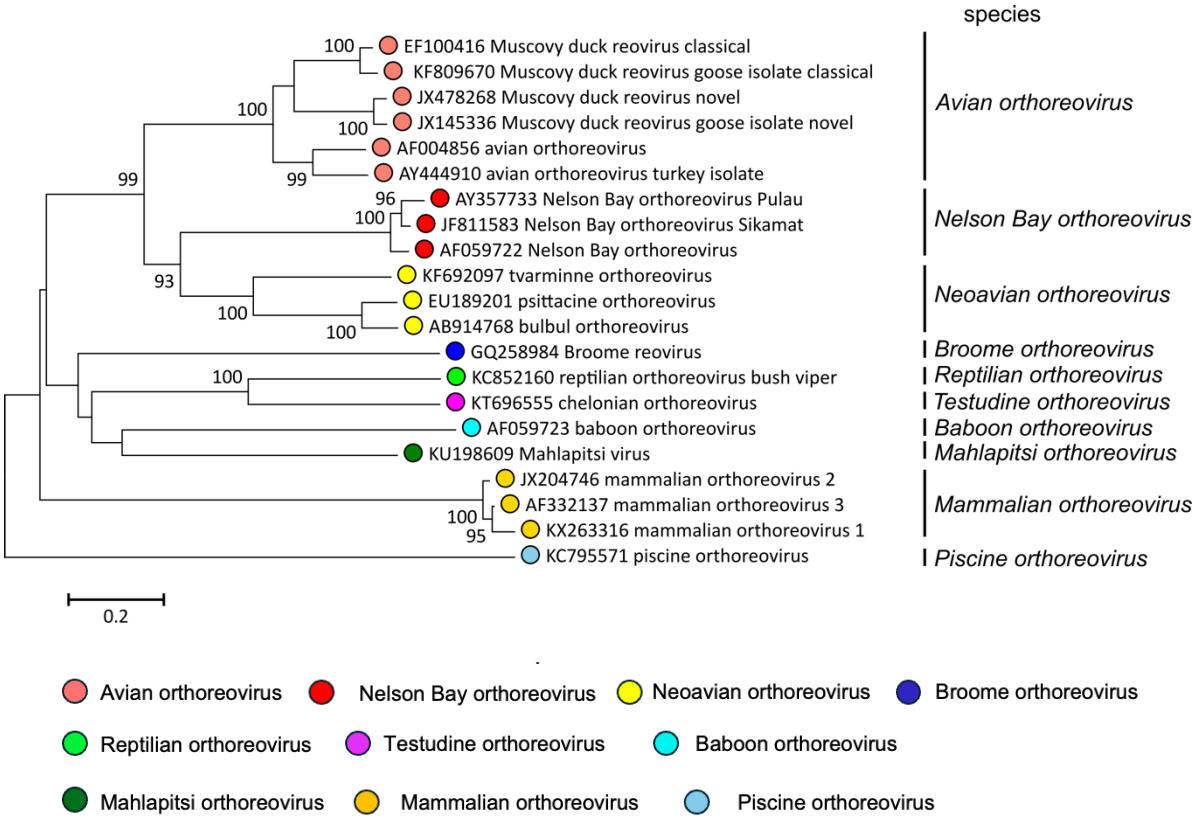

Figure 2. Evolutionary relationships of outer clamp protein of the 10 species of ORV.

The phylogenetic tree was obtained from https://ictv.global/report/chapter/spinareoviridae/spinareoviridae/orthoreovirus[41]

Chapter I:

Epidemiological study and characterization of Nelson Bay orthoreovirus (NBV) isolated from fruit bats in Indonesia

Summary

NBV is an emerging bat-borne virus and causes respiratory tract infections in humans sporadically. The NBV prototype strain was isolated from *Pteropus poliocephalus* in Nelson Bay, Australia, in 1968. Over the last two decades, several strains genetically related to NBV were isolated from humans and various bat species, predominantly in SEA, including Malaysia, Indonesia, and the Philippines, suggesting a high prevalence of NBV in this region. In this study, a new NBV strain was isolated from feces of IFBs collected in Paguyaman, tentatively named Paguyaman orthoreovirus (PgORV). Serological studies revealed that 81.2% (108/133) of IFB sera had neutralizing antibodies against PgORV. Whole-genome sequencing and phylogenetic analysis of PgORV suggested the occurrence of past reassortments with other NBV strains isolated in SEA, indicating the dispersal and circulation of NBVs among bats and humans in this region. PgORV replicated efficiently in human-derived cell lines and intranasal inoculation of mice with PgORV caused severe pneumonia with 62.5% mortality rate. This study demonstrated genetic background of PgORV and highlighted the potential risk of PgORV-related diseases in Indonesia.

Introduction

NBV is an emerging bat-borne virus that causes respiratory tract infection in humans[23-27]. The prototype NBV was isolated from the blood of *P. poliocephalus* collected in Nelson Bay, Australia in 1968, and the virus was designated as Nelson Bay virus[9]. Thereafter, several viruses genetically related to NBV have been reported from fruit bats and humans especially in SEA[14-15, 17-27].

Fruit bats belonging to the family *Pterodotidae* served as a natural reservior of NBV. NBVs were isolated from various species of fruit bats in Australia, Malaysia, Indonesia, Philippines, China, and Zambia where the Pteropodid bats distributed[9, 14-15, 17-27]. Among 18 strains of NBV discovered (Table 1), 13 strains have been isolated from fruit bats, respiratory tract infection patients, and macaques in SEA, indicating high prevalence of NBV in this region (Figure 3).

The first human NBV-infected case was reported from a 39-year-old male patient in 2006 in Melaka, Malaysia[27]. The patient had high-grade fever, headache, myalgia, mild cough, sore throat, and malaise. The virus belonging to NBV was isolated from his throat swab sample and was named Melaka virus (MelV). Epidemiological investigation revealed that 1 week before his illness, a bat flew to his living room while he was watching television, indicating possibility of NBV transmission from fruit bat to human. Several human cases were also reported later, particularly in Malaysia and Indonesia[23-27](Table 1.), and human-to-human transmission was evidenced in MelV, Kampar virus (KamV), and Sikamat virus infections[23, 26-27]. Furthermore, neutralizing antibodies to NBVs were detected in humans in Malaysia (2.2-17%), Singapore (0.8%), and Viet Nam (4.4%)[42-45]. These data indicated the emergence of NBV in the SEA region and highlighted the significance of NBV in public health.

Indonesia has the highest numbers of bat species in the world with approximately 225 bat species are hosting. As an archipelago country, the diverse ecosystems, tropical climate, and lush environment and foods make Indonesia become a good place for bats to thrive, especially fruit bats[46]. According to the previous studies, IFBs are carriers of many viruses, including herpesviruses, parvoviruses, polyomaviruses, paramyxoviruses, coronaviruses, and NBV[20, 22, 47-53]. Moreover, the incidence of NBV infections has been reported from one Japanese man and three Hong Kong travelers who visited Indonesia before clinical onset[24-25]. However, knowledge about the prevalence of NBVs in bats and humans in the country as well as the virological properties and zoonotic potential of NBVs are still insufficient and need to

be elucidated.

Previous studies established two members of NBV strains isolated from large flying foxes (*P. vampyrus*) captured in Indonesia, named Indonesia/2010 and Garut-69[20, 22]. In this study, a new member of NBV species was isolated from fruit bats in Indonesia, designated as PgORV. Viral genome characterization suggested the possibility of genetic reassortment events with other NBV strains. *In vitro* and *in vivo* characterization of PgORV demonstrated high growth efficiency in human-derived cell lines and intranasal inoculation of PgORV to laboratory mice caused severe pneumonia. Furthermore, the serological examination revealed a high prevalence of NBV infections in IFBs.

Table 1. Information of viruses belong to the NBV species

Year	Virus name	Host	Country of origin	Type of specimen
1968	Nelson Bay virus	Bat (*Pteropus policephalus*)	Australia	Blood
1999	Pulau virus	Bat (*Pteropus hypomelanus*)	Malaysia	Urine
2006	Melaka virus	Human	Malaysia	Throat swab
2006	Kampar virus	Human	Malaysia	Throat swab
2006	Xi river virus	Bat (*Rousettus leschenaultii*)	China	Lung tissue
2007	HK23629/07	Human	Indonesia	Throat and nasal swab
2007	Miyazaki Bali/2007	Human	Indonesia	Throat swab
2009	HK46886/09	Human	Indonesia	Throat and nasal swab
2010	HK50842/10	Human	Indonesia	Throat and nasal swab
2010	Sikamat	Human	Malaysia	Throat swab
2010	Indonesia/2010	Bat (*Pteropus vampyrus*)	Indonesia	Throat swab and feces
2012	Cangyuan virus	Bat (*Rousettus leschenaultii*)	China	Intestine
2013	Samal-24	Bat (*Eonycteris spelaea*)	Philippines	Throat swab
2013	Talikud-80	Bat (*Rousettus amplexicaudatus*)	Philippines	Throat swab
2013	Lopburi 01, 02	Macaque (*Macaca fascicularis*)	Thailand	Feces
2017	Garut-69	Bat (*Pteropus vampyrus*)	Indonesia	Rectal swab
2017	Kasama virus	Bat (*Lissonycteris angolensis ruwenzorii*)	Uganda	Rectal swab
2018	Nachunsulwe-57	Bat (*Rousettus aegyptiacus*)	Zambia	Colon

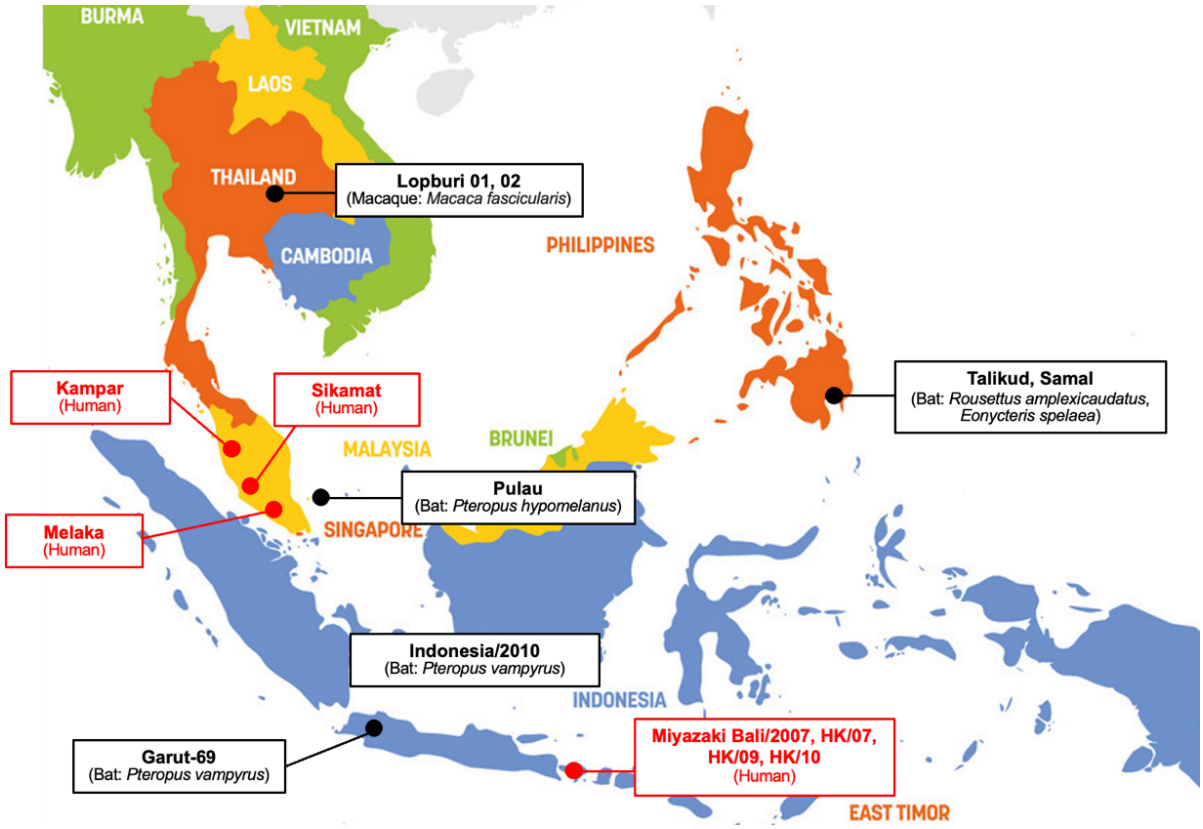

Figure 3. Geographical distribution of viruses belongs to NBV in SEA. Name of NBV strains and host species were indicated in the box. NBVs isolated from bats or macaques were presented in the black box, while the zoonotic strains isolated from humans were presented in the red box.

Materials and methods

Cells and viruses

Vero E6, Baby hamster kidney-21 (BHK-21), A549 cells were cultured and maintained in DMEM with 10% fetal bovine serum (FBS). Human embryonic kidney 293T (HEK293T) cells were grown in high glucose DMEM with 10% FBS, and Caco-2 cells were cultured in a collagen-coated plate in Dulbecco's modified eagle's medium (DMEM) supplemented with 10% FBS and 1% non-essential amino acid solution. Vero T2 cells, which were previously generated by Dr. Sasaki[54] and expressed human transmembrane protease serine 2 (TMPRSS2), were cultured using the same procedure as original Vero E6 cells. MB/07 strain[24] was propagated in HEK293T cells, while the newly isolated ORV, PgORV (ORV13-27) was propagated in Vero T2 cells. The virus stock was titrated by plaque assay using Vero E6 cells.

Bat samples and ethics statements

Blood, feces and organs were collected from IFBs in eight areas of Indonesia between 2010 and 2014 (Figure 4.). The samples were previously used for other virus screening[47-48, 50-53]. The Animal Care and Use Committee of Veterinary Teaching Hospital, IPB University approved the protocol for bat sampling (permit number 05-2010 RSHP-IPB). Collection and exportation of samples from fruit bats were performed under the permission of the Directorate General of Livestock and Animal Health Services, Ministry of Agriculture, Republic of Indonesia. As previously described, the bat species were identified by the external morphology and the nucleotide sequence analysis of 16S RNA and *cytochrome b* gene[53]. The Institutional Animal Care and Use Committee of Hokkaido University approved the ethics for the viral inoculation to laboratory animal experiments (approval number 20-0026).

Virus titration by plaque assay

Confluent monolayer of Vero E6 cells in 12-well plates were inoculated with a serially diluted virus and incubated for 1 hour for viral absorption with agitation at 37ºC. Then, the cells were overlaid with DMEM containing 2% FBS and 0.4% agar. After three days post-inoculation (dpi), the cells were fixed with 10% buffered formalin and stained with 1% crystal

violet. The viral titer was estimated as plaque-forming unit (pfu) based on the number of plaques.

Plaque reduction neutralization test (PRNT)

Sera from a total of 133 IFBs were heat-inactivated at 56°C for 30 min and serially diluted four-folds from 1: 10 to 1: 640. The diluted sera were mixed with an equal volume of DMEM with 2% FBS containing 100–200 pfu of either MB/07 or PgORV and incubated for 1 hour at 37°C. The mixture of the virus and serum (100 µl) was subjected to a plaque assay using Vero E6 cells as described above. Neutralizing antibody titers were determined as the highest dilution, which achieved more than 80% reduction in plaque numbers.

Screening of the ORV genome by nested RT-PCR

Total RNA was extracted from feces using a High Pure Viral Nucleic Acid Kit (Roche Diagnostics, Mannheim, Germany). Lungs were homogenized in TRIzol reagent (Invitrogen; Thermo Scientific, Waltham, USA) and subjected to ribonucleic acid (RNA) extraction using a Direct-Zol RNA MiniPrep kit (Zymo Research, Irvine, USA). The RNA samples were subjected to ORV screening by nested RT-PCR using two sets of degenerate primers targeting the ORV RNA-dependent RNA polymerase (RdRp) gene as described previously[55].

The first round RT-PCR was performed using 1607F primer (5′-CARMGNCGNSCH MGHTCHATHATGCC-3′), 2608R primer (5′-TAVAYRAAVGWCCASMHNGGRTAYTG-3′) and PrimeScript OneStep RT-PCR Kit Ver.2 (Takara Bio, Kusatsu, Japan). The second round PCR was performed with 2090F primer (5′-GGBTCMACNGCYACYTCBACYGAGCA-3′), 2334R primer (5′-CDATGTCRTAHWYCCANCCRAA-3′) and TaKaRa ExTaq Hot Start Version (Takara Bio). Amplicons at approximately 300 bp were subjected to sequencing using Big Dye Terminator v3.1 Cycle Sequencing Kit (Thermo Fisher Scientific, Waltham, USA).

Virus isolation

Fecal samples positive for the ORV genome were suspended in phosphate buffer saline (PBS) at 10% weight by volume (w/v). The suspensions were inoculated onto Vero T2 cells. Cells were maintained in serum-free DMEM supplemented with 2% antibiotic-antimycotic

solution (Wako, Osaka, Japan) and gentamicin (25 μg/ml). The culture supernatant was passaged into fresh monolayer cells after 5 dpi. The supernatants from wells showing cytopathic effect (CPE) were harvested and maintained at -80°C as a master stock of isolated viruses.

Whole-genome sequencing

Total RNA was extracted from five viral clones (ORV13-7, ORV13-8, ORV13-20, ORV13-25, and ORV13-27) and transcribed into double-stranded cDNA using PrimeScript Double Strand cDNA Synthesis Kit (Takara Bio). The sequence library was constructed using Nextera XT DNA Library Preparation Kit and sequenced on an Illumina MiSeq instrument (Illumina, San Diego, USA). The obtained sequence reads were assembled into contigs *via de novo* assembly or mapped to reference genome segments of MB/07 strain (GenBank accession; AB908278-AB908287) using CLC Genomics Workbench 20.1 (Qiagen, Venlo, Netherlands) and Geneious 2021.1.1 software (Biomatters, Auckland, New Zealand). Nucleotide sequences of ORV13-27 segments were deposited in the DNA Data Bank of Japan (DDBJ) with the accession numbers LC632072-LC632081.

Phylogenetic analysis

Reference nucleotide sequences of NBV species were obtained from the GenBank database and aligned with PgORV sequences. The best fit mathematical models for phylogenetic analyses of each segment were determined using MEGA 7 software[56]. Phylogenetic trees were constructed using the maximum likelihood (ML) method with 1,000 bootstrap replicates.

Replication efficiency in different cell lines

BHK-21, Vero E6, Vero T2, A549, Caco-2, and HEK293T cells were inoculated with PgORV at two different multiplicities of infection per cell (MOI = 0.01 or 0.0001) and maintained in culture media containing 2% FBS. Cell culture supernatants containing progeny viruses were harvested at 8, 24, 48, and 72 hours post-infection (hpi), and titrated by a plaque assay using Vero E6 cells.

Immunofluorescence assay (IFA)

Cells were seeded in a 24-well plate before inoculation with PgORV (ORV13-27, MOI = 0.01 or 0.0001). Cells were fixed with 10% buffered formalin at 14-hpi and permeabilized with 0.5% Triton X-100 in PBS. After blocking with 50% Block Ace (KAC, Kyoto, Japan), cells were incubated with self-made guinea pig anti-NBV Nachunsulwe-57 polyclonal antibody, which cross-reacted with PgORV[18] and Alexa 488-conjugated goat anti-guinea pig immunoglobulin G (IgG) (Invitrogen) as a secondary antibody. Cell nuclei were stained with Hoechst 33342 (Invitrogen) and the fluorescence signal was examined using a fluorescence microscope (IX73; Olympus, Tokyo, Japan).

Animal experiments

Male BALB/c mice (4-6-week-old, Japan SLC, Hamamatsu, Japan) were intranasally inoculated with PgORV (1×10^6 pfu of ORV13-27 in 50 µl PBS) or mock (50 µl PBS). Body weight (BW) was monitored daily up to 14 dpi and 20% BW loss was defined as a humane endpoint. To evaluate PgORV's growth and pathogenicity in laboratory mice, the lung was harvested at 1, 3, and 5 dpi for viral load measurement (n = 5) and histopathological examination (n = 3).

Measurement of the viral RNA load and cytokine gene expression in lung tissue

The lungs from mice experimentally infected with PgORV were homogenized in PBS at 10% w/v using TissueRuptor (Qiagen). Total RNA was extracted from the lung homogenates with TRIzol LS reagent and Direct-Zol RNA MiniPrep kit. Quantitative RT-PCR (qRT–PCR) assay was conducted using OneStep PrimeScript III RT–qPCR Mix (Takara Bio) with the primers and probe targeting the L1 segment of NBV species as described previously[57], TaqMan mouse β-actin (ACTB) Endogenous Control (Mm00607939_s1, Applied Biosystems; Thermo Fisher Scientific) or predesigned PrimeTime qPCR Assays for tumor necrosis factor (TNF) (Ms.PT.58.12575861), interferon-gamma (IFN-γ) (Ms.PT.58.41769240), interferon-beta (IFN-β) (Ms.PT.30132453.g), interleukin-6 (IL-6) (Ms.PT.58.10005566), the chemokine (C-C motif) ligand 2 (CCL2) (Ms.PT.58.42151692) and the chemokine (C-X-C motif) ligand 10 (CXCL10) (Ms.PT.58.43575827) (IDT, Coralville, USA). The levels of viral RNA and

cytokine gene expression were normalized to mouse ACTB and calculated the relative gene expression using $2^{-\Delta Ct}$ or $2^{-\Delta\Delta Ct}$ method[58].

Histopathology and immunohistochemistry (IHC)

Lungs from the PgORV-inoculated mice were fixed in 10% buffered formalin, embedded in paraffin blocks, and sectioned at 4 micrometers (μm). The sections were stained with Hematoxylin and Eosin (H&E) for histopathological examination. To detect PgORV antigen in lungs, the sections were deparaffinized and heated for 3 minutes in citrate buffer for antigen retrieval. The slides were blocked with 50% Block Ace and incubated with guinea pig anti-NBV Nachunsulwe-57 polyclonal antibody[18]. Immunostaining was visualized using VECTASTAIN ABC guinea pig IgG Kit (Vector laboratories, Burlingame, USA) and Histofine diaminobenzidine substrate kit (Nichirei Biosciences, Tokyo, Japan).

Statistical analysis

Data were analyzed and presented as the mean with standard deviation (SD). Statistical analysis was performed using Prism 8 (GraphPad Software, Boston, USA). Survival analysis was performed using Kaplan-Meier estimator. One-way analysis of variance (ANOVA) with Dunnett's test was used to determine the statistical significance of cytokine gene expression in the mouse lungs.

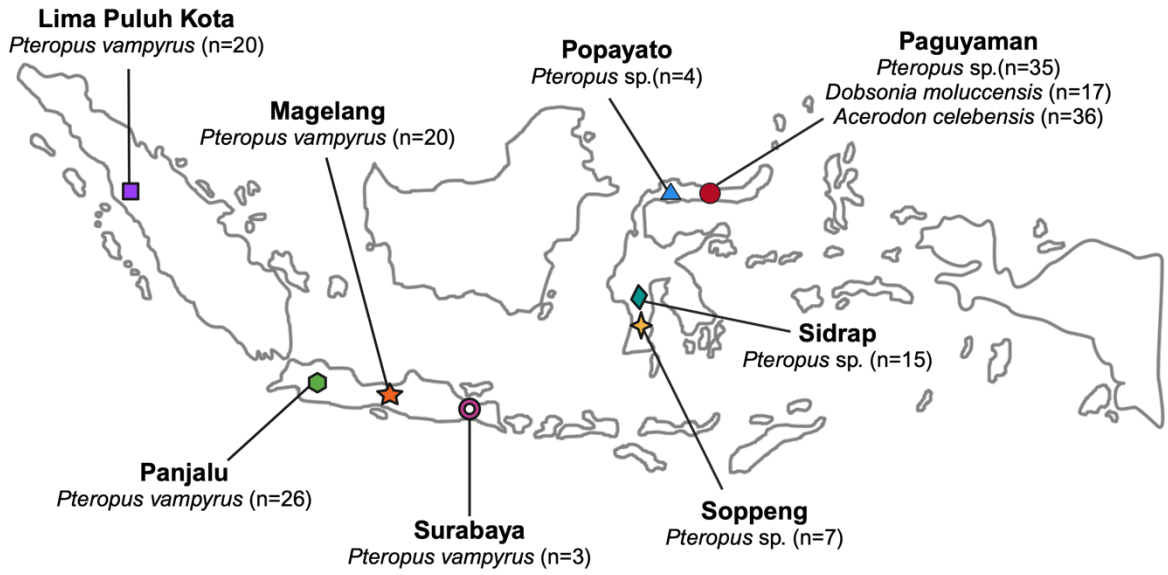

Figure 4. Locations of bat sampling in Indonesia from 2010-2014. The place where bat sampling was conducted, were indicated in the map of Indonesia. Bat species and total number of bats collected from 2010-2014 were also showed in each area. *Pteropus* sp. refer to bats that were genetically closely related to *Pteropus hypomelanus*.

Results

Screening and isolation of ORV in fruit bats in Indonesia

To investigate ORV infection among fruit bats in Indonesia, fecal (n=96) and lung (n=172) samples were examined for the *RdRp* gene of ORVs by nested RT-PCR method. The ORV genome was detected in the feces from *Pteropus* sp. (3/8) and *Acerodon celebensis* (3/7) collected in 2013, but not in the lungs (Table 2). Sequence analysis and basic local alignment search tool for nucleotide (BLASTn) search showed that the amplicons had high nucleotide sequence identity to the RdRp gene of NBV species.

Next, isolation of ORV from bat feces that were positive for ORV screening were performed. The fecal suspensions (n=6, sample ID: 13-7, 13-8, 13-9, 13-20, 13-25, and 13-27) were inoculated into Vero T2 cells. After the first blind passage, syncytium formation of cells which is the main characteristic of fusogenic ORV infection was observed in 5 of 6 inocula. The supernatants of cells that presented syncytium formation were harvested and confirmed that the isolated viruses were ORVs by RT-PCR and nucleotide sequencing of the ORV *RdRp* gene.

Table 2. Screening of ORV genome in IFBs

Year of sample collection	Location	Bat species	Number of positive samples	
			Lungs	Feces
2010	Panjalu	*Pteropus vampyrus*	0/15	NA[a]
2011	Lima Puluh Kota	*Pteropus vampyrus*	0/20	NA
	Paguyaman	*Pteropus* sp.[b]	0/23	NA
	Popayato	*Pteropus* sp.	0/4	NA
2012	Paguyaman	*Dobsonia moluccensis*	0/17	0/17
		Acerodon celebensis	0/18	0/18
		Pteropus sp.	0/2	0/2
	Surabaya	*Pteropus vampyrus*	0/3	0/3
	Magelang	*Pteropus vampyrus*	0/20	0/19
2013	Paguyaman	*Pteropus* sp.	0/10	3/8
		Acerodon celebensis	0/18	3/7
2014	Soppeng	*Pteropus* sp.	0/7	0/7
	Sidrap	*Pteropus* sp.	0/15	0/15
Total			**0/172**	**6/96**

[a] NA; sample not available
[b] *Pteropus* sp; bat genetically closely related to *Pteropus hypomelanus*

Whole-genome sequencing and phylogenetic analysis

To obtain full genome sequence of the five isolated viruses (designated as ORV13-7, ORV13-8, ORV13-20, ORV13-25, and ORV13-27), HTS was performed. The genome of the isolated viruses comprised of 10 genome segments. The putative complete sequences of 10 genome segments were identified by the terminal sequences of the 5′-untranslated region (5′-UTR) and the 3′-UTR (GCUUhh and UCAUC, respectively) that were conserved among the genus *Orthoreovirus* and the open reading frame (ORF). Sequence comparison of the five isolates displayed more than 99% nucleotide identity, indicating that all clones were the same virus strain. The isolated virus was designated as PgORV based on the location where the bat carrying the virus was captured. One clone (ORV13-27) was selected from the five clones as a representative strain of PgORV for further studies on genetic characterization, virological properties and pathogenicity.

Sequence analysis demonstrated that the putative complete genome of PgORV was 23,406 base pairs (bp) in length, and the lengths of the ten segments are shown in Table 3. All the segments except for S1 encode only one protein (monocistronic), but the PgORV S1 segment encodes three viral proteins (tricistronic) (Table 3). Pairwise comparison of 10 genome segments of PgORV with the known NBV revealed that L1, L3, M1–M3, and S4 segments shared the highest nucleotide sequence identities with those of MB/07, while L2 and S3 displayed 89.1% and 93.6% nucleotide sequence identity with the NBVs isolated from fruit bats in Philippines: Talikud-74 and Samal-24, respectively (Table 3). The nucleotide sequence of the S1 segment was highly similar to Sikamat strain which was isolated from human in Malaysia (84.5% identity), whereas S2 segment had 89.6% identity to the prototype NBV strain (Table 3).

Phylogenetic analysis showed that these PgORV segments formed clusters with humans and bats NBV strains originated in Indonesia, including MB/07, Indonesia/2010, Garut-69, HK23629/07 (HK/07), HK46886/09 (HK/09), and HK50842/10 (HK/10) strains (Figure 5)[20, 22, 24-25]. Conversely, L2, S2, and S3 segments of PgORV were closely related to Talikud and Samal strains isolated from fruit bats in the Philippines[17]. S1 was the most genetically divergent among the segments, and phylogenetic analysis showed that the PgORV-S1 segment shared the same ancestor with the zoonotic NBV strains reported in Malaysia (Sikamat and MelV) and NBV strains detected from macaques in Thailand (Lopburi 01 and Lopburi 02)[26-27, 59] (Figure 5).

Table 3. Molecular characteristics of ORV isolated from IFB (ORV13-27)

Genome segment	Accession No.	Size (bp)	Terminal sequences		Encoded protein(s)	Closest strain (% nucleotide identity)	Host
			5' UTR	3' UTR			
L1	LC632072	3896	GCUUUA	UCAUC	λC	Miyazaki-Bali/2007 (98.2)	Human
L2	LC632073	3832	GCUUUA	UCAUC	λB	Talikud-74 (89.1)	Bat
L3	LC632074	3954	GCUUUA	UCAUC	λA	Miyazaki-Bali/2007 (93.4)	Human
M1	LC632075	2295	GCUUUA	UCAUC	μA	Miyazaki-Bali/2007 (94.7)	Human
M2	LC632076	2145	GCUUAU	UCAUC	μB	Miyazaki-Bali/2007 (96.5)	Human
M3	LC632077	1984	GCUUAU	UCAUC	μNS	Miyazaki-Bali/2007 (96.4)	Human
S1	LC632078	1602	GCUUAA	UCAUC	p10, p17, σC	Sikamat (84.5)	Human
S2	LC632079	1322	GCUUAA	UCAUC	σA	Nelson bay virus (89.6)	Bat
S3	LC632080	1192	GCUUAU	UCAUC	σNS	Samal-24 (93.6)	Bat
S4	LC632081	1184	GCUUAU	UCAUC	σB	Miyazaki-Bali/2007 (96.6)	Human

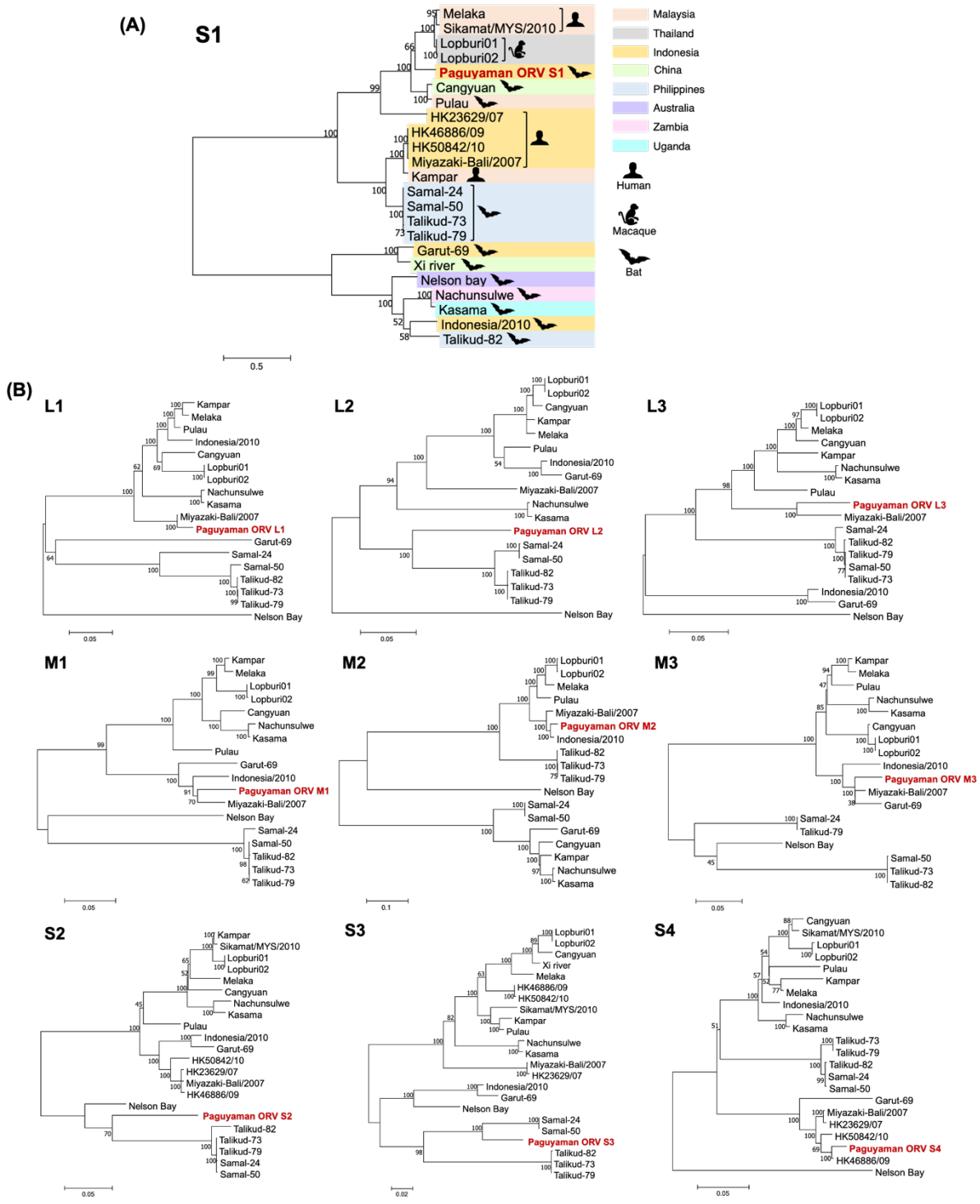

Figure 5. Phylogenetic analysis of PgORV. (A and B) Nucleotide sequences of 10 genome segments (L1-L3, M1-M3 and S1–S4) of reference ORVs and PgORV were aligned. Phylogenetic trees of S1 segment (A) and other segments (B) were constructed using the ML method. Bootstrap values of 1,000 replicates are shown in each node and the scale bars represent the number of nucleotide substitutions per site. The host which the virus was

identified, is shown in the phylogenetic tree of S1 segment (A). Each color indicates the country where the virus was identified (A).

Seroprevalence of NBVs in IFBs

To determine seroprevalence of NBVs in IFBs, neutralizing antibodies to MB/07 and PgORV were examined in sera of fruit bats by $PRNT_{80}$. Among 133 serum samples, 118 (89.5%) and 108 (81.2%) had neutralizing activities against MB/07 and PgORV, respectively (Table 4). Neutralizing titers were ranged between 1:20 to 1:1280 and seropositive bats were identified from *P. vampyrus* (100% to MB/07 and 93.6% to PgORV), *Pteropus* sp. (100% to MB/07 and 90.5% to PgORV), *Dobsonia moluccensis* (100% to MB/07 and 100% to PgORV), and *Acerodon celebensis* (50% to MB/07 and 35.7% to PgORV) (Table 4 and Figure 6). Notably, the seropositive rate of PgORV was slightly lower than that of MB/07 (Table 4). Most bat sera showed neutralizing activities against both PgORV and MB/07, suggesting a possible cross-neutralization between these NBV members (Figure 6). However, 57.9% (77/133) of bat sera exhibited a higher neutralizing titer against MB/07 than PgORV (Table 4 and Figure 6).

Table 4. Neutralizing antibodies to MB/07 and PgORV in IFBs

Year of sample collection	Location	Bat species	Neutralization titer to MB/07					Number of positive samples (%)	Neutralization titer to PgORV					Number of positive samples (%)
			0	20	80	320	1280		0	20	80	320	1280	
2010	Panjalu	*Pteropus vampyrus*	0	1	5	7	2	15/15 (100)	1	4	6	3	1	14/15 (93.3)
2011	Lima Puluh Kota	*Pteropus vampyrus*	0	0	4	4	2	10/10 (100)	0	1	6	3	0	10/10 (100)
	Paguyaman	*Pteropus* sp.[a]	0	4	4	5	5	18/18 (100)	2	6	5	2	3	16/18 (88.9)
	Popayato	*Pteropus* sp.	0	0	0	1	2	3/3 (100)	0	0	0	1	2	3/3 (100)
2012	Paguyaman	*Dobsonia moluccensis*	0	0	7	6	3	16/16 (100)	0	2	6	8	0	16/16 (100)
		Acerodon celebensis	9	2	4	2	1	9/18 (50)	10	6	2	0	0	8/18 (44.4)
		Pteropus sp.	0	0	0	2	0	2/2 (100)	0	2	0	0	0	2/2 (100)
	Surabaya	*Pteropus vampyrus*	0	0	1	0	2	3/3 (100)	0	1	0	0	2	3/3 (100)
	Magelang	*Pteropus vampyrus*	0	3	3	5	8	19/19 (100)	2	5	6	4	2	17/19 (89.5)
2013	Paguyaman	*Pteropus* sp.	0	0	1	6	3	10/10 (100)	1	0	7	2	0	9/10 (90)
		Acerodon celebensis	5	2	2	1	0	5/10 (50)	8	1	1	0	0	2/10 (20)
2014	Soppeng	*Pteropus* sp.	0	0	0	3	3	6/6 (100)	1	1	3	1	0	5/6 (83.3)
	Sidrap	*Pteropus* sp.	0	0	0	1	2	3/3 (100)	0	2	1	0	0	3/3 (100)
Total			**14**	**12**	**31**	**43**	**33**	**119/133 (89.5)**	**25**	**31**	**43**	**24**	**10**	**108/133 (81.2)**

[a] *Pteropus* Sp.; bat genetically closely related to *Pteropus hypomelanus*

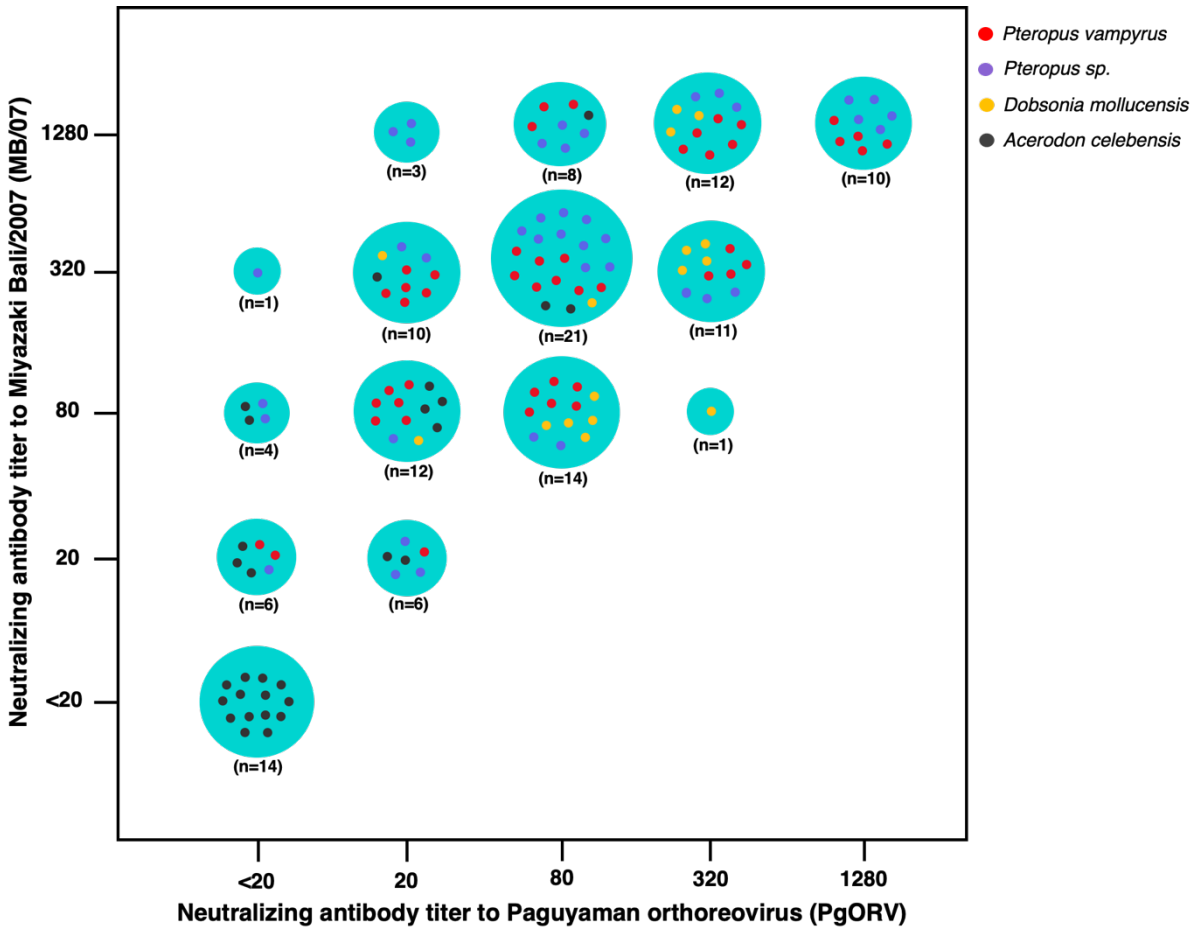

Figure 6. Serum neutralizing antibody titers to MB/07 and PgORV of IFBs. A total 133 of bat sera were examined by $PRNT_{80}$. Each dot represents neutralization antibody titer to both strains of each serum sample. The color refers bat species as follows; red; *P. vampyrus*, purple; *Pteropus* sp. (genetically closely related to *Pteropus hypomelanus*), yellow; *Dobsonia moluccensis* and gray; *Acerodon celebensis*. The number of positive serum samples at the indicated titer was shown in parentheses.

Growth properties of PgORV in cell lines

To investigate cell tropism of PgORV, infectivity and growth kinetics of PgORV were characterized *in vitro* using various cell lines. Viral infectivity was determined by IFA using convalescent serum from a guinea pig infected with NBV Nachunsulwe-57 strain that cross-reacted with PgORV antigens[18]. IFA analysis showed that all examined cell lines were susceptible to the infection with PgORV at an MOI of 0.01 (Figure 7A). Morphologically, distinct syncytia formations were observed in BHK-21, Vero E6, and Vero T2 cells, but Caco-2 and HEK293T cells formed huge syncytia after inoculated with PgORV. The virus titers in the supernatants of BHK-21, Vero E6, and Vero T2 cells increased in time-dependent manner (Figure 7B). In contrast, the virus titers in A549, Caco-2, and HEK293T cells peaked at 24 or 48 hpi, presumably due to CPE and cell detachment by PgORV infection. To observe the multi-cycle of viral infection in A549, Caco-2, and HEK293T cells, cells were inoculated with PgORV at an MOI of 0.0001. Infected cells were scarcely observed in BHK-21, Vero E6, and Vero T2 cells, but A549, HEK293T, and Caco-2 cells were highly sensitive to the infection even at the lower MOI (Figure 7C). The virus titers in the supernatants of A549, HEK293T, and Caco-2 cells also time-dependently increased, and the HEK293T cells had the highest progeny virus production (Figure 7D).

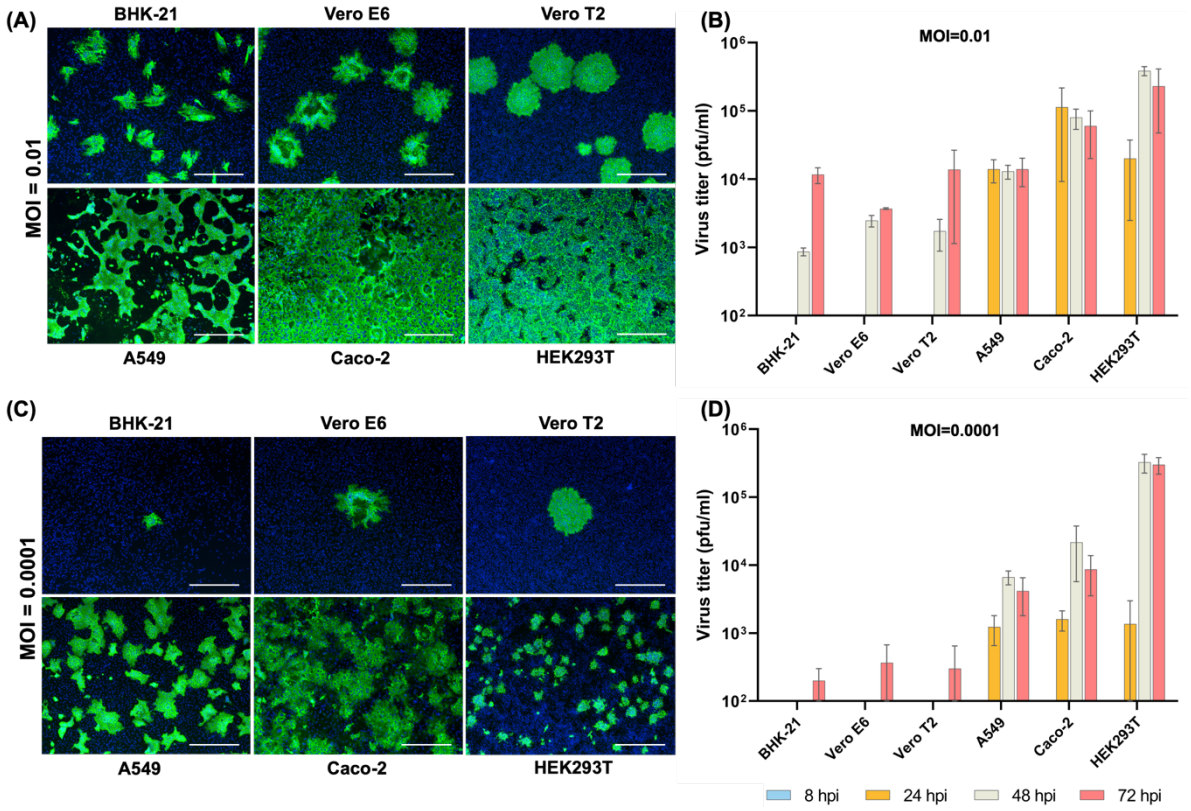

Figure 7. Infectivity and growth of PgORV in cell lines. Detection of PgORV infection by immunofluorescence staining (A, C). Cells were inoculated with the virus at MOIs of 0.01 and 0.0001 and fixed at 14 hours post infection. The cells were stained with guinea pig anti-NBV (Nachunsulwe-57) polyclonal antibody for PgORV (green) and Hoechst 33342 for cell nucleus (blue) (scale bars: 500 μm). (B, D) Cells were inoculated with PgORV at MOIs of 0.01 and 0.0001. Virus titers in cell culture supernatants at the indicated time points were determined by plaque assay.

Pathogenicity of PgORV in laboratory mice

Pathogenicity of NBVs in laboratory mice varies from low to high pathogenic depending on the virus strain. To investigate pathogenicity of PgORV, BALB/c mice were inoculated with the virus (1×10^6 pfu) *via* the intranasal route. The mice were monitored daily for BW changes and lungs were collected to examine viral titer and histopathological changes (Figure 8A). The BW of mice inoculated with PgORV continuously decreased from 1dpi to 4 dpi and some mice recovered from the infection by rebounding their BW (Figure 8B). In this study, 5 out of 8 mice inoculated with PgORV reached an endpoint due to severe BW loss more than 20% at 4 and 6 dpi, evoked 62.5% mortality rate (Figure 8C). The other three mice recovered and survived from the infection. The viral titer and viral RNA level in the lungs were quantified using plaque assay and qRT–PCR, respectively. The peak of viral titer was observed in the lung of mice at 1 dpi, and the titer decreased in time-dependent manner (Figure 8D). Similarly, the viral RNA load was also highest at 1 dpi and gradually decreased (Figure 8E).

Additionally, histopathological changes in the lungs after PgORV inoculation was examined at 1, 3 and 5 dpi. Gross examination of the lungs of mice inoculated with PgORV exhibited congestion and hyperemia at 3 and 5 dpi (Figure 9A). Histopathological findings revealed hemorrhage and infiltration of inflammatory cells in lungs at 1, 3, and 5 dpi, and massive infiltration of inflammatory cells was observed at 5 dpi (Figure 9B). Viral antigens were detected in bronchial and alveolar epithelial cells of mice inoculated with PgORV at 1 and 3 dpi by IHC; however, little IHC signal was detected at 5 dpi (Figure 9C). The severity of pneumonia conversely correlated with decreased of viral load, as indicated by IHC, qRT-PCR, and plaque assay. These results implied that the host immune responses to the infection eliminated the virus in the lung but caused severe inflammation.

To investigate the host immune responses against PgORV infection, the expression levels of inflammatory cytokine genes in PgORV-inoculated mice lungs were examined using qRT-PCR. The levels of pro-inflammatory cytokines, including TNF, IFN-β, and IL-6 as well as chemoattractants (CCL2 and CXCL2), were significantly increased in PgORV-infected mice lungs at 1 dpi, indicating the early host responses to viral infection. Contrastly, IFN-γ, which influences viral clearance, was significantly upregulated in mice lungs at 5 dpi (Figure 9D), supporting the hypothesis of the viral clearance by host immune responses in mice.

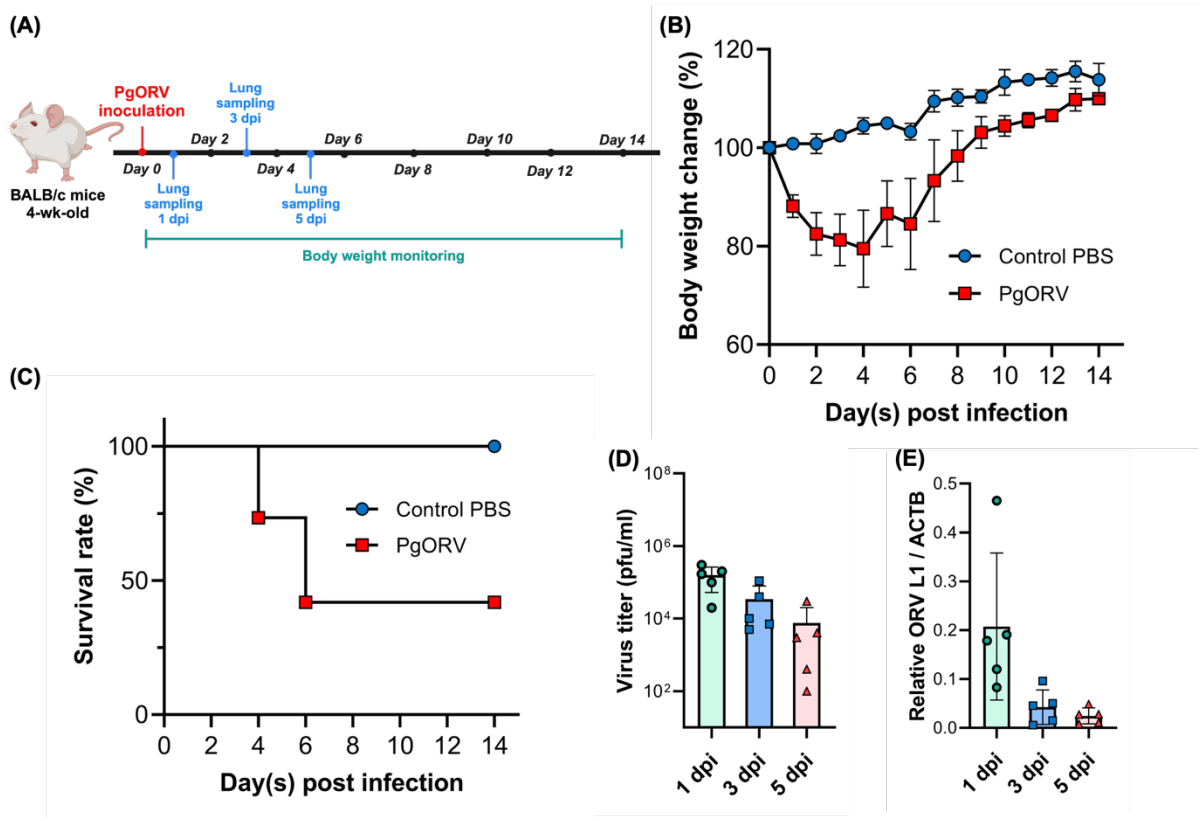

Figure 8. Infection of laboratory mice with PgORV. (A) The scheme of experimental infection in BALB/c mice. Mice were intranasally infected with 1×10^6 pfu of PgORV or PBS as control. (B) The average percentage of BW changes of mice after PgORV infection. (C) Survival rate of mice infected with PgORV. A humane endpoint was applied when the mice showed more than 20% BW loss. (D) Virus titer in the lung at the indicated time points were determined by plaque assay. (E) Viral RNA levels in the lungs were normalized to the mRNA levels of mouse ACTB and the relative expression of L1 gene was calculated by $2^{-\Delta Ct}$ method.

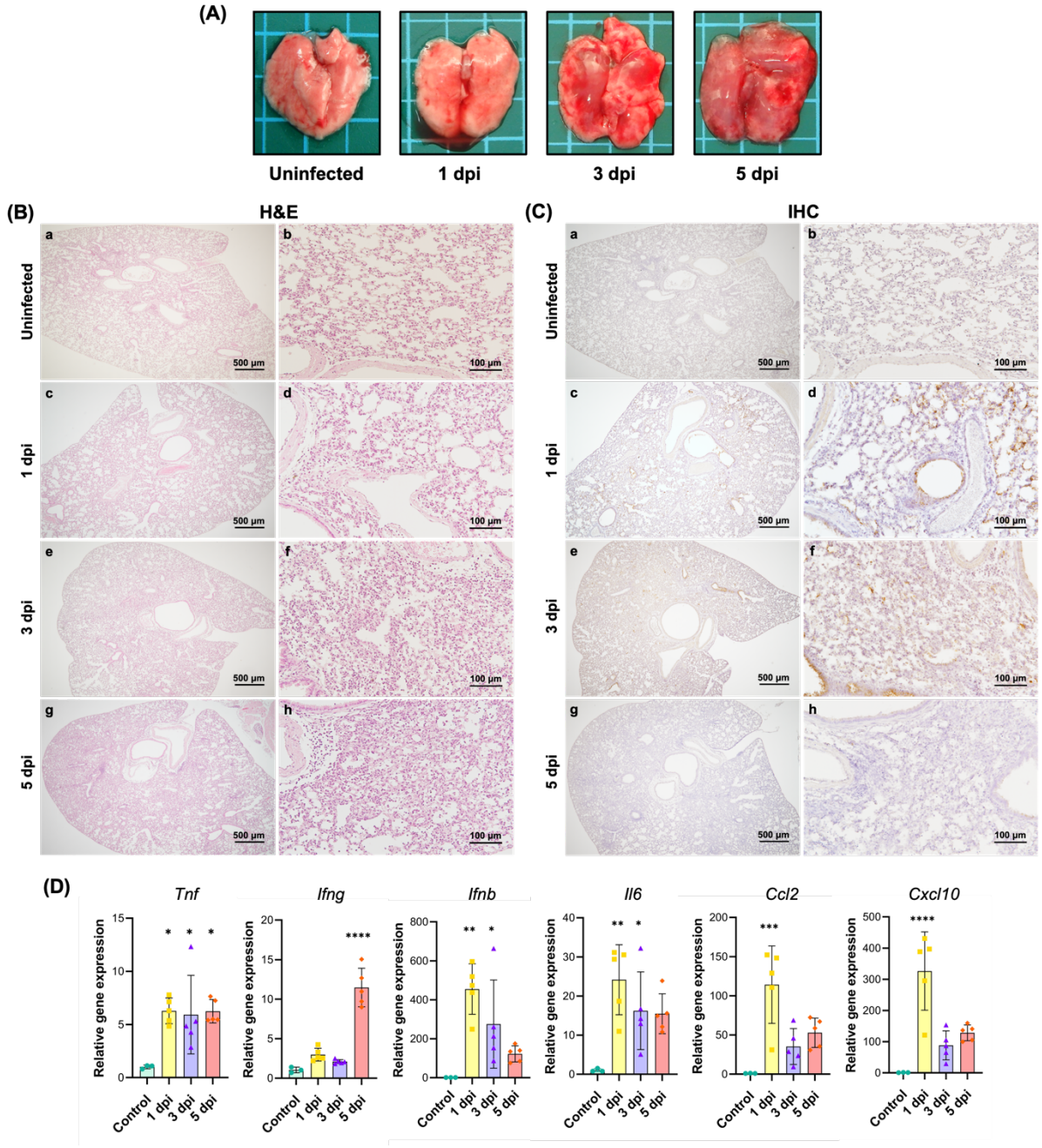

Figure 9. Pathological change and cytokine expression profile in the lung of mice infected with PgORV. BALB/c mice were infected intranasally with 1×10^6 pfu of PgORV. (A) Macroscopic appearances of mice lungs after infection. (B) H&E staining of the lung sections. (C) Detection of PgORV antigen in the lungs by IHC. Lung sections were stained with guinea pig anti-NBV (Nachunsulwe-57) polyclonal antibody and counterstained of cell nuclei with Hematoxylin. Scale bars of the left panels (a, c, e, g): 500 μm, right panels (b, d, f, h): 100 μm. (D) Cytokine expression levels in the mice lungs. Data were normalized to mouse ACTB and the relative gene expression level of each cytokine was calculated by $2^{-\Delta\Delta Ct}$ method. One-way ANOVA with Dunnett's test was used to determine the statistical significance of differences

between uninfected control and infected mice. *, $p < 0.05$; **, $p < 0.01$, ***, $p < 0.001$; ****, $p < 0.0001$.

Discussion

Since NBV discovery, several NBV strains have been identified from fruit bats[9, 14, 17-22]. Approximately 70% of NBV strains were isolated in SEA countries, indicating a high NBV prevalence in this region. Currently, six NBV strains, including HK/07, HK/09, HK/10, MB/07, Indonesia/2010, and Garut-69, have been reported in Indonesia[20, 22, 24-25]. Three HK strains and MB/07 were isolated from the respiratory tract specimens of patients who had a history of visiting Indonesia before the onset of influenza-like symptoms[24-25]. Garut-69 was isolated from *P. vampyrus* in West Java Island[22]. Indonesia/2010 strain was also isolated from *P. vampyrus* that were imported to Italy from Indonesia; however, there was no information on sampling sites of bats from which the virus was detected[20]. In this study, NBV seropositive bats were observed in West Sumatra (Lima Puluh Kota), West Java (Panjalu, Magelang, and Surabaya), North Sulawesi (Popayato and Paguyaman), and South Sulawesi (Soppeng and Sidrap), indicating a broad dispersal of NBV infection among IFBs.

L1, L3, M1, M2, M3, and S4 segments of PgORV showed high nucleotide sequence identities (93.4-98.2%) with MB/07, suggesting that PgORV and MB/07 evolved from a common ancestor. However, the remaining L2, S1, S2, and S3 segments of PgORV were phylogenetically distant from those of MB/07 and related to other NBVs. This phylogenetic incongruence suggests genetic reassortments between NBVs in fruit bats, reported in several studies[15, 17, 19-20, 22, 59]. The fact that bats can fly long distances and move between islands and countries, may contribute to a long-distance dispersal and genetic reassortment of ORVs[60-62].

Previous studies reported that 26, 83, and 98% of fruit bats were NBV seropositive in China, Philippines, and Zambia, respectively[17-19]. Similarly, this study revealed that 81.2–89.5% of IFB sera had neutralizing antibodies against NBVs. Bats are highly diversified with over 1,400 species worldwide and almost 200 species of fruit bats. Various fruit bat species, including *P. poliocephalus*, *P. hypomelanus*, *Rousettus leschenautia, R. amplexicaudatus*, *R. aegyptiacus*, *Eonycteris spelaea*, *Macroglossus minimus*, *Lissonycteris angolensis ruwenzorii,* and *Eidolon helvum,* were evidenced for NBV infections[9, 14-15, 17-22]. In this study, the antibodies to NBV were newly detected in *Acerodon celebensis* and *Dobsonia moluccensis*.

Neutralization antibody to NBV was developed mainly against cell attachment protein (σC) encoded by S1 segment[63]. In addition, neutralizing activities may be generated against outer capsid protein (σB) encoded by S4 segment and turret protein (λC) encoded by L1 segment[63]. Cross-neutralization has been observed in several strains of NBV species. Antisera

to the prototype NBV cross-reacts with Pulau (PuV), MelV, and KamV[26]. Antisera against MB/07 has also shown the cross-reactivity to NBVs of Samal-24, Talikud-82 and Nachunsulwe-57[17, 18]. In this study, IFBs had a high seropositivity to both PgORV and MB/07. Among NBV members, PgORV was phylogenetically close to MB/07; therefore, it was supposed that the antibodies could cross-react between these two NBV strains. Additionally, the PRNT assays showed that a subset of bat sera exhibited higher neutralizing activity to MB/07 strain than PgORV, suggesting that these bats would be exposed to MB/07 or MB/07-related NBV rather than PgORV. For these reasons, the possibility of cross-reactivity between PgORV and known/unknown NBV members cannot be excluded in this PRNT result.

After replication in host cells, the virus spreads to adjacent cells via two modes; cell-free and cell-to-cell transmissions[64-66]. The multinuclear syncytium is a characteristic of cells infected with PgORV. The IFA detected the syncytia with PgORV antigen in BHK-21, Vero E6, and Vero T2 cells at 14 hpi. However, the progeny virus titers in the culture supernatant of these cell lines were under the detection limit at 24 hpi. These results suggest that the primary spreading mode of PgORV is cell-to-cell mechanism. Consistent with the studies of MB/07, Samal-24, and Garut-50[17, 67], human-derived cell lines, including A549, Caco-2, and HEK293T, were highly susceptible to PgORV infection. Although Vero T2 cells were employed for virus isolation, using A549, Caco-2, and HEK293T cells could be a better outcome for NBV isolation.

The mortality rate of PgORV-inoculated mice (62.5%) was lower than that of MB/07-inoculated mice (100%), indicating that MB/07 is more pathogenic than PgORV in mice[68-69]. Similar to MB/07 and Samal-24 infections[68], PgORV infection caused severe pneumonia in mice lungs. Hemorrhage and infiltration of inflammatory cells were massively present in the lungs at 3 and 5 dpi, while cells positive for viral antigen were abundant at 1 dpi and subsequently decreased at 3 and 5 dpi, indicating PgORV clearance from the host. The manifestation of PgORV-infected mice was uncorrelated with the viral load in the lungs. This discrepancy is observed in mouse models infected with influenza, respiratory syncytial, and coronaviruses[70-72]. The expression levels of pro-inflammatory cytokines (TNF, IFN-β, and IL-6) and chemoattractants (CCL2 and CXCL10) were significantly upregulated at 1 dpi for the initial responses to viral infection, subsequent recruitment of inflammatory cells causing the induction of IFN-γ expression. TNF and IFN-γ influence virus clearance and causes immunopathology[73-74].

In conclusion, PgORV which was isolated from IFBs can cause respiratory disease in mammals. Serological study in IFBs also demonstrated a high seroprevalence of NBVs in multiple species of fruit bats in different areas of Indonesia. This study emphasizes the broad distribution and circulation of NBV among fruit bats in Indonesia. Further investigations in bats, other animals, and humans should be conducted to evaluate the current burden and the zoonotic potential of NBVs in Indonesia.

Chapter II:

Characterization of a mammalian orthoreovirus (MRV) isolated from a large flying fox; *Pteropus vampyrus* in Indonesia

Summary

Fruit bats serve as an important reservoir for many zoonotic pathogens, including Nipah virus, Hendra virus, Marburg virus and lyssavirus. To gain a deeper insight into the virological characteristics, pathogenicity and zoonotic potential of bat-borne viruses, recovery of infectious viruses from field samples is important. In this study, the first MRV strain was isolated and reported from a large flying fox *(P. vampyrus)* in Indonesia and SEA. MRV was recovered from fecal samples of three different *P. vampyrus* in Central Java. Nucleotide sequence analysis revealed that the genome of the three MRV isolates shared more than 99% nucleotide sequence identity to each other. One of the isolated viruses, MRV12-52 was used for further analysis and characterization. Among 10 genome segments, MRV12-52 S1 and S4 which encode the cell-attachment protein and outer capsid protein, had 93.6 and 95.3% nucleotide sequence identities with known MRV strains, respectively. Meanwhile the remaining genome segments of MRV12-52 were divergent with 73-80% nucleotide sequence identities to the known MRVs. Based on the nucleotide sequence of the S1 segment, MRV12-52 was grouped into serotype 2, and phylogenetic analysis demonstrated evidence of past reassortment events. *In vitro* characterization of MRV12-52 showed that the virus efficiently replicated in BHK-21, HEK293T, and A549 cells. In addition, experimental infection of laboratory mice with MRV12-52 caused severe pneumonia with 75% mortality. This study highlights the presence of pathogenic MRV in Indonesia which could serve as a potential animal and public health concern.

Introduction

MRV was the first identified species of ORV and has been detected in a broad range of mammalian hosts, including humans, livestock, bats, and wildlife[10-13, 28-40, 75-81]. Moreover, MRV can persist in the environment and is frequently detected in sewage[82-83]. Based on neutralization activities of the cell attachment protein encoded by the S1 segment, MRVs can be classified into 4 serotypes: Type 1 Lang, Type 2 Jones, Type 3 Dearing, and Type 4 Ndelle[84-86].

MRVs cause a variety of diseases depending on the host and virus strains. In humans, MRV infection results in asymptomatic, mild acute gastroenteritis, or mild upper respiratory tract infection[35-37]. Occasionally, MRV can cause meningitis and encephalitis in children[37-39]. In animal, MRV serotype 3 causes diarrhea and respiratory distress in pigs that affects their production and subsequent to economic loss[76-77].

MRVs have been identified and isolated from various species of insectivorous bats in China, Japan, South Korea, Slovenia, Germany, Italy, Canada and USA[10-13, 29-34]. Bat MRVs displayed diverse genetic backgrounds and are classified into serotypes 1-3[10-13, 28-34]. Genomic reassortment events occur in segmented viruses and are important in viral evolution and the emergence of virus reassortment strains. Most bat MRV genomes are related to those detected in humans, pigs, and wildlife, suggesting cross-species transmission of the virus among these hosts, and is the basis for reassortment of genome segments with the other MRV strains[10-13, 87-89]. Although many bat MRVs are closely related to human MRVs, evidence for spillover from bats to humans is still largely unknown. Only one MRV strain (SI-MRV01) which was highly similar to the MRV strain isolated from a bat in Germany (342/08) has been reported from an infant with gastroenteritis in Slovenia[35]. Therefore, the knowledge on genetic diversity, virological properties, and zoonotic potential of bat MRV need to be further elucidated.

There have been several reports on identification of herpesviruses, parvoviruses, polyomaviruses, paramyxoviruses, coronaviruses, and NBV from IFBs[20, 22, 47-53]. Among these viruses, infectious herpesvirus and NBV were recovered from tissues and feces of the bats[47, 90]. In the present study, a cultured cell-based approach was conducted to identify infectious viruses, and MRV was successfully isolated from fecal samples of large flying fox (*P. vampyrus*) collected in Central Java, Indonesia. To characterize the genetic and virological properties of the isolated MRV, whole genome sequence, growth efficiency in cell lines, and pathogenicity of a representative isolate (MRV12-52) in laboratory mice were examined.

Materials and Methods

Bat sampling and animal ethics statement

Bat sampling was performed in Sumatra (Lima Puluh Kota), Java (Panjalu, Magelang and Surabaya) and Sulawesi (Popayato, Paguyaman, Sidrap and Soppeng), in Indonesia from 2010 to 2014 (Figure 4) under permit number 05-2010 RSHP-IPB approved by the Animal Care and Use Committee of Veterinary Teaching Hospital, Bogor Agricultural University. Samples were collected from bats and were exported under the permission of the Directorate General of Livestock and Animal Health Services, Ministry of Agriculture, Republic of Indonesia. All samples were kept at -80^{o}C and used for virus screening as described previously[53].

Cells and viruses

Vero E6, Vero T2, Vero T2-expressing human angiotensin converting enzyme-2 (ACE2) (Vero T2-hACE2) and A549 cells were cultured and maintained in DMEM with 10% FBS. Caco-2 cells were grown in DMEM supplemented with 1% non-essential amino acid and 10% FBS in a collagen-coated plate, and HEK293T cells were cultured in high glucose DMEM with 10% FBS. BHK-21 cells were grown and maintained in Minimum Essential Medium (MEM) supplemented with 10%FBS.

To facilitate SARS betacoronavirus (Sarbecovirus) isolation in IFBs, Vero T2-expressing *Acerodon celebensis* ACE2 (Vero T2-AcACE2) and Vero T2-expressing *Dobsonia moluccensis* ACE2 (Vero T2-DmACE2) were generated by lentiviral transduction system. In brief, full-length of bat ACE2 genes were transduced into pLVSIN-EF1α Pur plasmid. Vero T2 cells were transfected with the lentiviral vector plasmid and Lentiviral High Titer Packaging Mix (Takara Bio, Shiga, Japan) and cultured in the presence of puromycin for selection of cells expressing the plasmid. Vero T2 cells expressing bat ACE2 were cultured and maintained in the same condition as Vero E6. All cell lines were cultured at 37^{o}C with 5% CO_2.

The isolated viruses (MRV12-47, MRV12-48, and MRV12-52) were propagated in Vero T2-hACE2 or BHK-21 and the virus stocks were titrated by 50% tissue culture infectious dose ($TCID_{50}$) or focus forming assay (FFA) using BHK-21 cells.

Virus isolation

Fecal and lung samples of fruit bats were suspended in PBS at 10% w/v and homogenized using beads as described previously[90]. Throat swab samples were collected from bats and kept in 1 ml of viral transport medium. The samples were centrifuged at 6,000 x *g* for 3 minutes and supernatants were filtered using Vivaclear mini clarifying filter 0.8 μm (Sartorius, Stonehouse, UK). Vero T2-AcACE2, Vero T2-DmACE2, and Vero T2-hACE2 cultured in 12-well plates were inoculated with 20 μl of the suspensions. Cells were maintained in DMEM supplemented with 2% FBS, 2% antibiotic-antimycotic solution and gentamicin (25 μg/ml). Blind passage was performed twice after 7 days of culture. Cells were monitored daily for the appearance of CPE and the supernatants from cells showing CPE was collected and kept at -80°C as master stocks of the isolated viruses.

Identification of virus morphology by electron microscopy

The isolated viruses were propagated in Vero T2-hACE2 cells and pelleted by ultracentrifugation at 110,800 x *g* for 1.5 hours with a 20% sucrose cushion and resuspended in PBS. The virus particles were fixed with 4% paraformaldehyde, loaded onto polyvinyl-coated nickel grids (Nissin EM, Tokyo, Japan) and negatively stained with 2% phosphotungstic acid solution (pH 5.8). The morphology of the isolated viruses was observed under a transmission electron microscope (TEM) Hitachi HT7800 (Hitachi Ltd., Ibaraki, Japan).

Full-genome sequencing

Total RNAs were extracted from the culture supernatants of cells infected with MRV12-47, MRV12-48, and MRV12-52 with a High Pure Viral Nucleic Acid kit (Roche Diagnostics) and reverse transcribed into a double-strand cDNA using PrimeScript Double Strand cDNA Synthesis Kit (Takara Bio). The sequence library was constructed using Nextera XT DNA Library Preparation Kit and sequenced on an Illumina MiSeq instrument (Illumina).

Sequence and phylogenetic analysis

The contigs of viral genome segments were generated by *de novo* assembly and mapped to reads approach using CLC Genomics Workbench 20.1 (Qiagen). For phylogenetic analysis,

coding nucleotide sequences of the reference MRVs were obtained from the GenBank database. The reference sequences were aligned with MRV12-47, MRV12-48, and MRV12-52 sequences using MUSCLE alignment[91]. The best fit mathematical model for each segment was tested using MEGA11 software[56] and the model which has the lowest Bayesian information criterion (BIC) value was chosen. The mathematical model of general time-reversible (GTR) with gamma distributed (G) and invariant sites (I) was used for construction of ML tree of L1-L3, M1, M2 and S3, while the Tamura-Nei model with G+I was used to construct the phylogenetic tree of M3, GTR+G was used for the S1 and S2 trees, and Kimura 2 with G was used for the S4 tree. The algorithm was analyzed with a bootstrapping value of 1,000 replicates. The trees were visualized using the Interactive Tree of Life (iTOL) version 6.8.1[92].

Production of anti-MRV polyclonal antibody

Female Hartley guinea pigs (5-week-old, Japan SLC Inc.) were intranasally inoculated with 2.5 x 10^6 $TCID_{50}$ of MRV12-52. The animals were boosted twice with the same dose *via* intraperitoneal injection at 2 and 4 weeks after the first immunization. At 42 dpi, the animals were euthanized by excessive isoflurane inhalation and blood was collected *via* cardiac puncture. After heat-inactivation at 56°C for 30 min, the sera were stored at -80 °C and used as anti-MRV12-52 polyclonal antibody for virus titration by FFA, IFA, and IHC.

Virus titration by FFA

The specimens were 10-fold serially diluted and inoculated onto monolayers of BHK-21 cells cultured in 24-well plates. The plates were incubated at 37°C for 1 hour and then cultured in DMEM containing 2% FBS and 0.8% methylcellulose. Cells were fixed with 10% buffered formalin at 36 hpi. Cells were blocked with 50% Block Ace in PBS and then stained with 1:3,000 of guinea pig anti-MRV12-52 antibody and Alexa-Fluor 488-conjugated goat anti-guinea pig IgG (Invitrogen) as a secondary antibody. Cell nuclei were stained with Hoescht 33342 (Invitrogen). Viral antigen-positive foci were counted under a fluorescence microscope (IX73, Olympus). Virus titers were calculated as focus-forming units per milliliter (ffu/ml) based on the number of foci.

Growth kinetics and IFA staining of MRV12-52 in cell lines

Vero E6, Vero T2, Vero T2-hACE2, BHK-21, A549, Caco-2 and HEK293T cells cultured in 12 well-plates were inoculated with MRV12-52 at an MOI of 0.01. Cell culture supernatants were collected at 0, 24, 48 and 72 hpi and subjected to titration by FFA as described above.

For IFA, cells were inoculated with MRV12-52 at an MOI of 0.01 and cultured in maintenance media supplemented with 2% FBS. Cells were fixed at 48 hpi and stained with the same protocol as FFA. The merged images were prepared using CellSens Imaging Software (Olympus).

Animal experiments

Female BALB/c mice (4-week-old, Japan SLC Inc.) were intranasally inoculated with 10^6 ffu of MRV12-52 in 50 µl PBS or PBS only as mock infection. For survival analysis, the BW was monitored daily up to 14 dpi. The humane endpoint was established as BW loss exceeding 20%. For virus quantification, five mice were sacrificed at 1, 3, 5, and 7 dpi, and the organs, including lung, liver, spleen, kidney and intestine were harvested in 3 ml of PBS. The lungs were collected in 10% buffered formalin from 3 mice at 3, 5, and 7 dpi for histopathological examination.

Animal experiments with MRV had ethical approval from the Institutional Animal Care and Use Committee of Hokkaido University (approval number 20-0026).

Virus quantification in the organs of mice

The organs from mice were homogenized in PBS using a TissueRuptor (Qiagen). To examine viral RNA levels, total RNAs were extracted from homogenized lung, liver, spleen, kidney and intestine with TRIzol LS reagent (Invitrogen) and Direct-Zol RNA MiniPrep kit (Zymo Research). qRT–PCR assay was performed with THUNDERBIRD Probe One-step qRT-PCR Kit (TOYOBO, Osaka, Japan). Primer and probe sequences for MRV12-52 L2 segment were 5′–CCCGCGACTCCTGTATTATTC–3′, 5′–CACTGCCGACGATACTTCATA G–3′ and 5′–FAM–CGTCGCCTC-ZEN-ATGTGTGTC–IBFQ–3′. The expression levels of endogenous mouse ACTB were quantified for normalization with Taqman mouse ACTB

Endogenous Control (Mm00607939_s1, Applied Biosystems). The relative gene expression of the L2 segment was calculated by $2^{-\Delta Ct}$ method.

To determine viral titers in organs, homogenized tissues were cleared by centrifugation and titrated by FFA as described above.

Histopathological examination

The fixed lungs were processed for paraffin embedding and sectioned at 3 μm. The lung sections were deparaffinized and stained with H&E for histopathological examination. For IHC, the sections were deparaffinized and heated in citrate buffer for 3 minutes using a pressure cooker for antigen retrieval. The sections were stained with guinea pig anti-MRV12-52 polyclonal antibody, anti-cluster of differentiation 3 (CD3) (ab16669; Abcam, Cambridge, UK), anti-ionized calcium binding adaptor molecule 1 (Iba1) (019-19741, Fujifilm-Wako, Osaka, Japan) or anti-myeloperoxidase (MPO) (A039829-2; Dako; Agilent, Santa Clara, CA). Immunostaining was detected with the EnVision system peroxidase-labeled anti-rabbit immunoglobulin (Dako; Agilent) or VECTASTAIN ABC guinea pig IgG Kit (Vector laboratories) and then visualized using a Histofine diaminobenzidine substrate kit (Nichirei Biosciences).

Statistical analysis

Data were analyzed and presented as the mean with SD. Statistical analysis was performed using GraphPad Prism 8 software (Biomatters). Survival analysis was performed using the Kaplan-Meier estimator. One-way ANOVA with Dunnett's test was used to determine the statistical significance of gene expression in the mouse lungs. Two-way ANOVA with Turkey's multiple comparisons was used to compare statistical differences between viral titers in Vero E6, Vero T2, and Vero T2-hACE2 cells at each time point.

Results

Virus isolation from IFBs and morphological identification

At the beginning of this study, sarbecovirus was intended to be isolated from IFBs using Vero cells co-expressing TMPRSS2 and bat or human ACE2. Supernatants from homogenized lungs, feces, and throat swabs of IFBs were inoculated into Vero T2-AcACE2, Vero T2-DmACE2, and Vero T2-hACE2 cells. After the 2nd blind passage, CPEs with cell rounding and detachment were observed in Vero T2-hACE2 cells inoculated with fecal samples (ID: IFB12-47, IFB12-48, and IFB12-52) that were collected from *P. vampyrus* in Magelang, Central Java in 2012 (Figure 10A and Table 5). The morphology of the isolated virus was examined by TEM. Virus particles were approximately 80 nanometers (nm) in diameter, had a spherical wheel-liked shape, and exhibited a double-layered capsids, which are the typical characteristics of reovirus (Figure 10B).

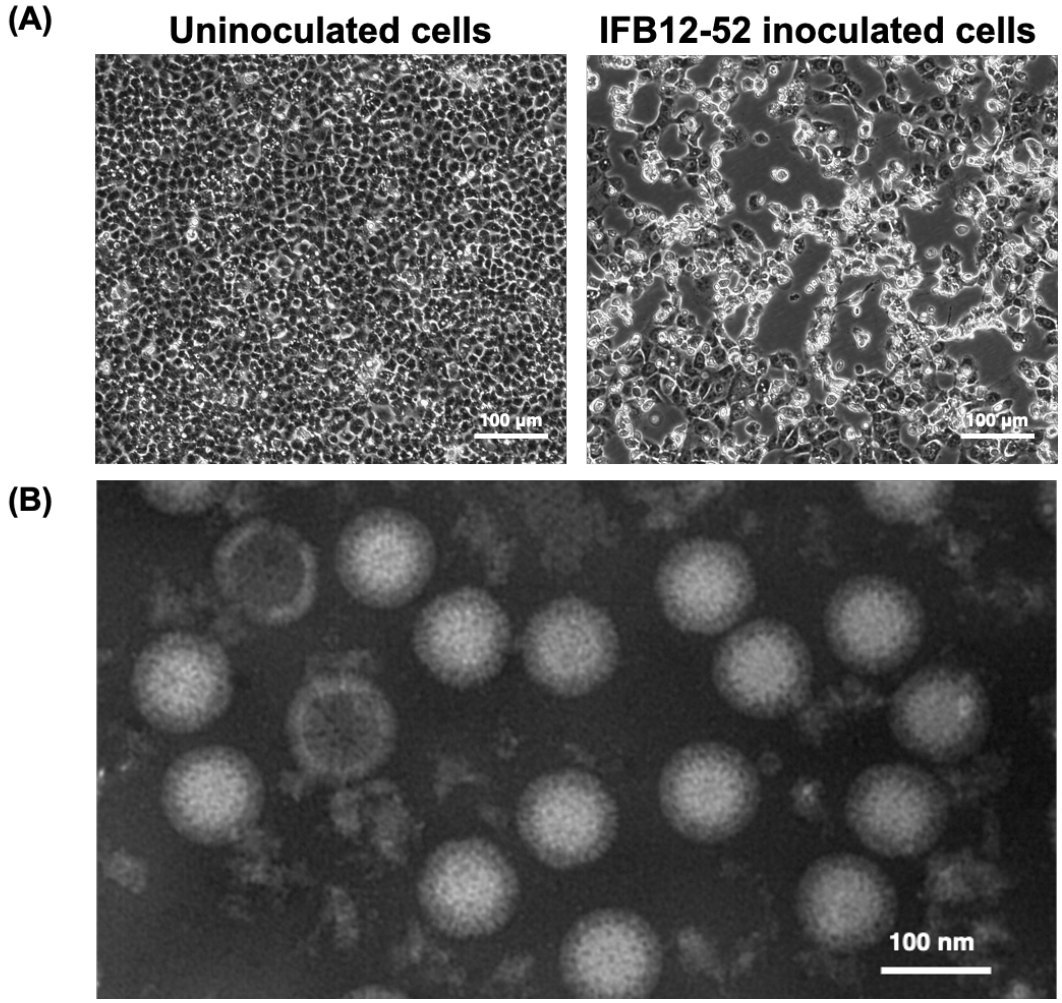

Figure 10. CPEs and virion morphology of MRV from IFB. (A) Vero T2-hACE2 cells were inoculated with mock (left panel) or a fecal suspension of IFB12-52 at 5 dpi. Scale bar = 100 μm. (B) Negatively stained electron micrograph of the isolated virus by TEM. Scale bar = 100 nm.

Table 5. Results of virus isolation from specimens of IFBs

Location	Region	Year	Bat species	Virus isolation (positive/total)		
				Lung	Throat swab	Feces
Panjalu	West Java	2010	*Pteropus vampyrus*	0/15	NA[a]	NA
Lima Puluh Kota	West Sumatra	2011	*Pteropus vampyrus*	0/20	NA	NA
Popayato	North Sulawesi	2011	*Pteropus* sp.[b]	0/4	NA	NA
Paguyaman	North Sulawesi	2011	*Pteropus* sp.	0/23	NA	NA
		2012	*Pteropus* sp.	0/2	NA	0/2
			Dobsonia moluccensis	0/17	NA	0/17
			Acerodon celebensis	0/18	NA	0/18
		2013	*Pteropus* sp.	0/8	0/8	0/6
			Acerodon celebensis	0/15	0/15	0/4
Surabaya	East Java	2012	*Pteropus vampyrus*	0/3	NA	0/3
Magelang	Central Java	2012	*Pteropus vampyrus*	0/20	NA	3/19
Soppeng	South Sulawesi	2014	*Pteropus* sp.	0/7	0/7	0/7
Sidrap	South Sulawesi	2014	*Pteropus* sp.	0/15	0/15	0/15
Total				**0/167**	**0/45**	**3/91**

[a] NA; sample not available
[b] *Pteropus* sp.; bat genetically closely related to *Pteropus hypomelanus*

39

Genetic characterization and phylogenetic analysis of the isolated viruses

Full-genome sequencing was performed using HTS. According to the National Center for Biotechnology Information (NCBI) BLASTn searches, the nucleotide sequences of the isolated viruses were highly similar to those of MRVs. The putative complete genome sequences consisting of the coding region and the termini of 10 genome segments were obtained from the culture supernatants of Vero T2-hACE2 cells inoculated with feces of IFB12-47, IFB12-48, and IFB12-52. The three isolated viruses were designated as MRV12-47, MRV12-48, and MRV12-52. Nucleotide sequences of the 10 segments were deposited in DDBJ with accession numbers LC773568-LC773597. A pairwise comparison of each genome segment of the three isolates showed more than 99% identity to each other, indicating that all isolates are the same virus.

In this study, MRV12-52 was chosen as a representative isolate for further characterization. Whole genome of MRV12-52 consisted of 10 segments: L1, 3,854 bp; L2, 3,915 bp; L3, 3,901 bp; M1, 2,304 bp; M2, 2,203 bp; M3, 2,241 bp; S1, 1,437 bp; S2, 1,331 bp; S3, 1,198 bp and S4, 1,197 bp (Table 6). A pairwise comparison of 10 genome segments of MRV12-52 to the other known MRV strains by BLASTn demonstrated diverse nucleotide sequence identities ranging from 73.3 to 95.3% (Table 6). Gene encoding core structures including L1-L3, M1-M3, S2, and S3 had low sequence identities (73.3 to 80.8%) to known MRV strains isolated from pig, bat, human, and mink (Tables 6 and 7). In contrast, the gene encoding the attachment protein (S1) was highly similar to that of MRV serotype 2 strain OV204 which was isolated from deer in the USA (93.6% identity)[81]. The gene encoding a major outer-capsid protein (S4) showed 95.3% nucleotide sequence identity with Osaka 1994 strain, which was isolated from an infant with meningitis in Japan[37].

L-class, M-class, S2, and S3 segments of the isolated MRVs formed distinct lineages from the other MRVs (Figures 11 and 12), while S1 and S4 segments were assigned to the same cluster with the other MRVs (Figure 12). MRVs can be classified into 4 serotypes based on the nucleotide sequence of the S1 segment. Phylogenetic analysis of the S1 segment demonstrated that MRV12-47, MRV12-48 and MRV12-52 were assigned to serotype 2 (Figure 12).

Analysis of MRV12-52 genome exhibited diverse coding nucleotide and amino acid sequences with the other MRV strains (Table 7). The C-terminal domain in the core non-structural protein μNS encoded by M3 is essential to form inclusions termed a virus factory-like structure (VFL)[93]. Notably, MRV12-52 also had a highly divergent of amino acid sequence

in this domain (Figure 13). These results highlighted the unique genetic background of MRVs isolated from IFBs.

Table 6. Pairwise comparison of 10 genome segments of MRV12-52 with the known MRV strains

Genome segment	Protein	Sequence length (bp)	MRVs with highest nucleotide identity (Accession No.)	Identity (%)	Host	Country
L1	Core (RdRp)	3854	Mammalian orthoreovirus 2 strain CH/GX/PReoV/2435 (MZ298655)	77.2	Pig	China
L2	Core (Turret)	3915	Mammalian orthoreovirus 1 strain Kansas 40 (OP057408)	75.7	Bat	USA
L3	Core (Shell)	3901	Mammalian orthoreovirus 2 strain SI-MRV08 (MT518186)	77.8	Human	Slovenia
M1	Core (NTPase)	2304	Mammalian orthoreovirus 2 strain RpMRV-YN2012 (KM087108)	73.3	Bat	China
M2	Outer shell	2203	Mammalian orthoreovirus 3 strain SD-14 (KT224508)	80.8	Mink	China
M3	NS	2241	Mammalian orthoreovirus 1 strain Kansas 40 (OP057406)	74.8	Bat	USA
S1	Attachment protein	1437	Mammalian orthoreovirus 2 strain OV204 (MK092970)	93.6	Deer	USA
S2	Core clamp	1331	Mammalian orthoreovirus 2 Jones (L19775)	79.4	Human	USA
S3	NS	1198	Mammalian orthoreovirus 3 strain 4476 (MN233077)	79.3	Pig	USA
S4	Outer capsid	1197	Mammalian orthoreovirus 2 Osaka 1994 (LC476904)	95.3	Human	Japan

Table 7. Pairwise comparison of coding nucleotide sequence and amino acid sequence of MRV12-52 with the prototype, human, pig, bat, and wildlife MRVs

	Nucleotide (amino acid) sequence identities											
	Prototype strains				Human		Pig		Bat		Wildlife	
MRV12-52	Lang	Jones	Dearing	Ndelle	SI-MRV08	Osaka 1994	4476	CH/Gx/PReo	Kansas40	YN2012	SD-14	OV204
L1 (λ3)	75.8 (91.9)	74.5 (91.0)	75.8 (92.4)	75.6 (91.9)	73.9 (91.1)	76.5 (92.7)	76.0 (92.3)	76.7 (92.9)	76.6 (92.5)	76.0 (92.7)	76.4 (92.8)	76.4 (92.7)
L2 (λ2)	73.3 (88.1)	73.0 (87.3)	75.2 (89.5)	NA[a]	73.0 (87.0)	73.5 (88.1)	73.8 (87.4)	73.6 (87.4)	75.3 (89.1)	74.6 (89.4)	73.4 (88.3)	73.1 (88.3)
L3 (λ1)	77.1 (96.1)	77.4 (95.5)	76.8 (96.1)	NA	77.5 (95.3)	77.3 (96.6)	76.7 (95.9)	77.1 (96.0)	77.3 (96.6)	77.2 (96.0)	77.4 (96.7)	77.2 (96.8)
M1 (μ2)	72.9 (82.9)	71.4 (80.6)	72.6 (82.5)	NA	69.9 (80.0)	72.4 (82.5)	72.1 (82.3)	71.6 (81.7)	72.6 (82.7)	71.9 (81.9)	71.9 (82.3)	72.1 (83.6)
M2 (μ2)	79.0 (97.6)	78.2 (97.2)	79.0 (97.0)	79.3 (98.2)	77.8 (96.9)	80.3 (97.5)	79.0 (97.0)	78.9 (96.6)	79.3 (97.7)	80.2 (97.0)	80.7 (97.7)	80.3 (97.6)
M3 (μNS)	72.7 (83.8)	70.5 (80.3)	72.2 (83.8)	NA	71.6 (80.8)	72.8 (83.9)	71.6 (83.1)	72.6 (82.9)	72.9 (83.1)	72.8 (83.9)	72.2 (83.9)	71.7 (83.1)
S1 (σ1)	57.1 (51.8)	61.7 (62.8)	38.0 (25.7)	37.2 (24.2)	60.1 (60.8)	70.8 (74.6)	36.9 (24.5)	65.3 (68.8)	56.9 (52.2)	91.6 (95.2)	38.0 (21.3)	93.6 (97.0)
S2 (σ2)	77.7 (95.9)	77.2 (94.3)	78.5 (95.5)	76.7 (94.0)	77.5 (93.8)	76.8 (95.7)	76.7 (95.2)	77.1 (95.5)	77.7 (95.9)	77.5 (95.7)	77.0 (95.9)	76.1 (95.9)
S3 (σNS)	77.5 (89.6)	74.8 (86.1)	76.1 (89.9)	NA	74.8 (87.2)	77.2 (90.4)	77.8 (91.0)	76.5 (90.4)	76.7 (90.2)	77.8 (91.0)	77.2 (90.2)	76.3 (89.6)
S4 (σ3)	87.0 (96.2)	80.0 (91.2)	87.5 (96.4)	89.7 (95.8)	80.4 (90.7)	95.1 (98.4)	76.2 (86.0)	77.5 (85.8)	92.5 (97.0)	91.1 (97.3)	93.6 (97.8)	93.7 (97.8)

[a] NA; sequence not available

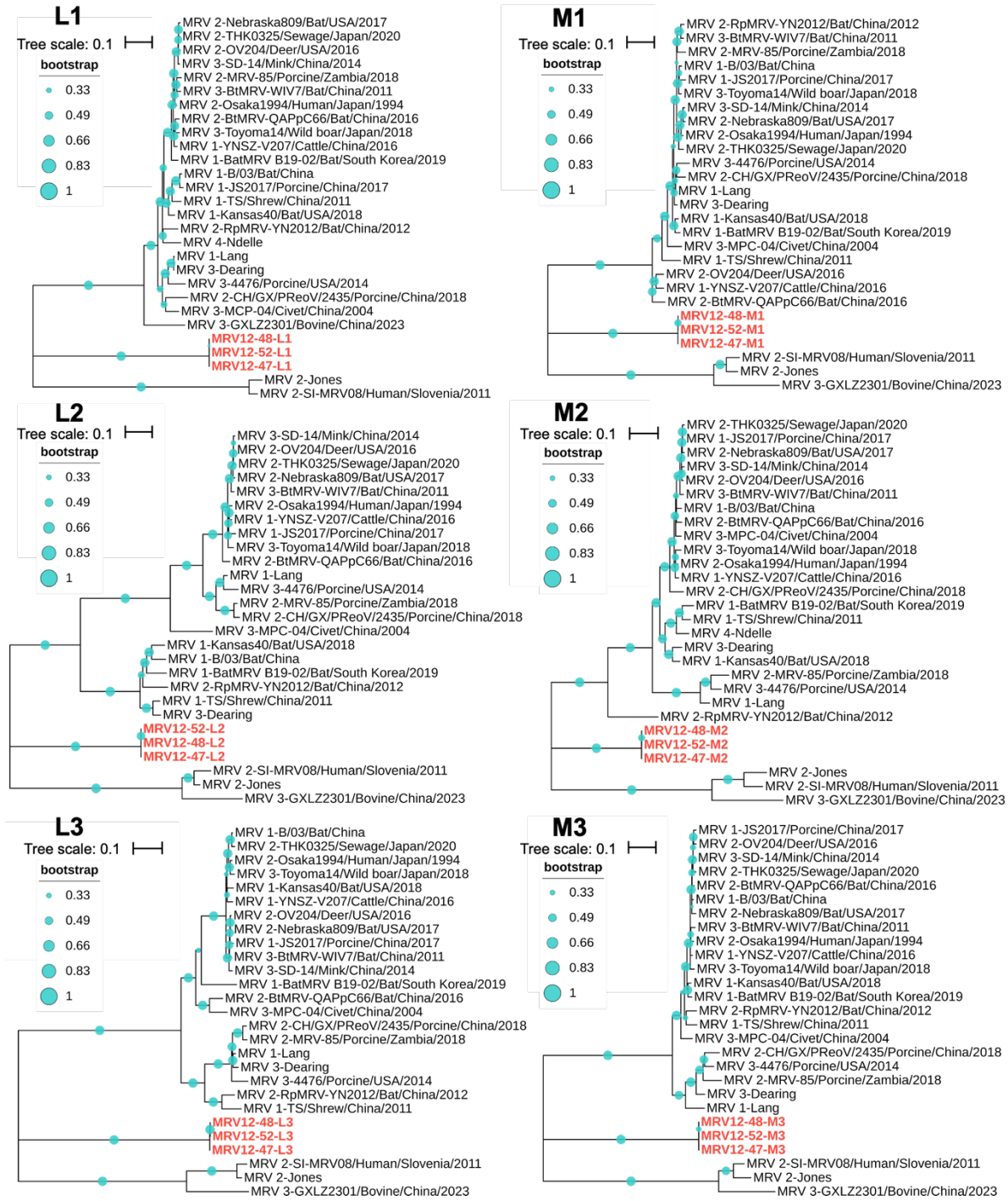

Figure 11. Phylogenetic analysis of large (L) and medium (M) genome segments of the isolated MRVs. Coding nucleotide sequences of L1, L2, L3, M1, M2, and M3 segments of the reference MRVs, MRV12-47, MRV12-48, and MRV12-52 were aligned. Phylogenetic trees of each segment were constructed using the ML method with bootstrap values of 1,000 replicates. The bootstrap values were indicated as a decimal number represented by a green circle. The scale bars represent the number of nucleotide substitutions per site.

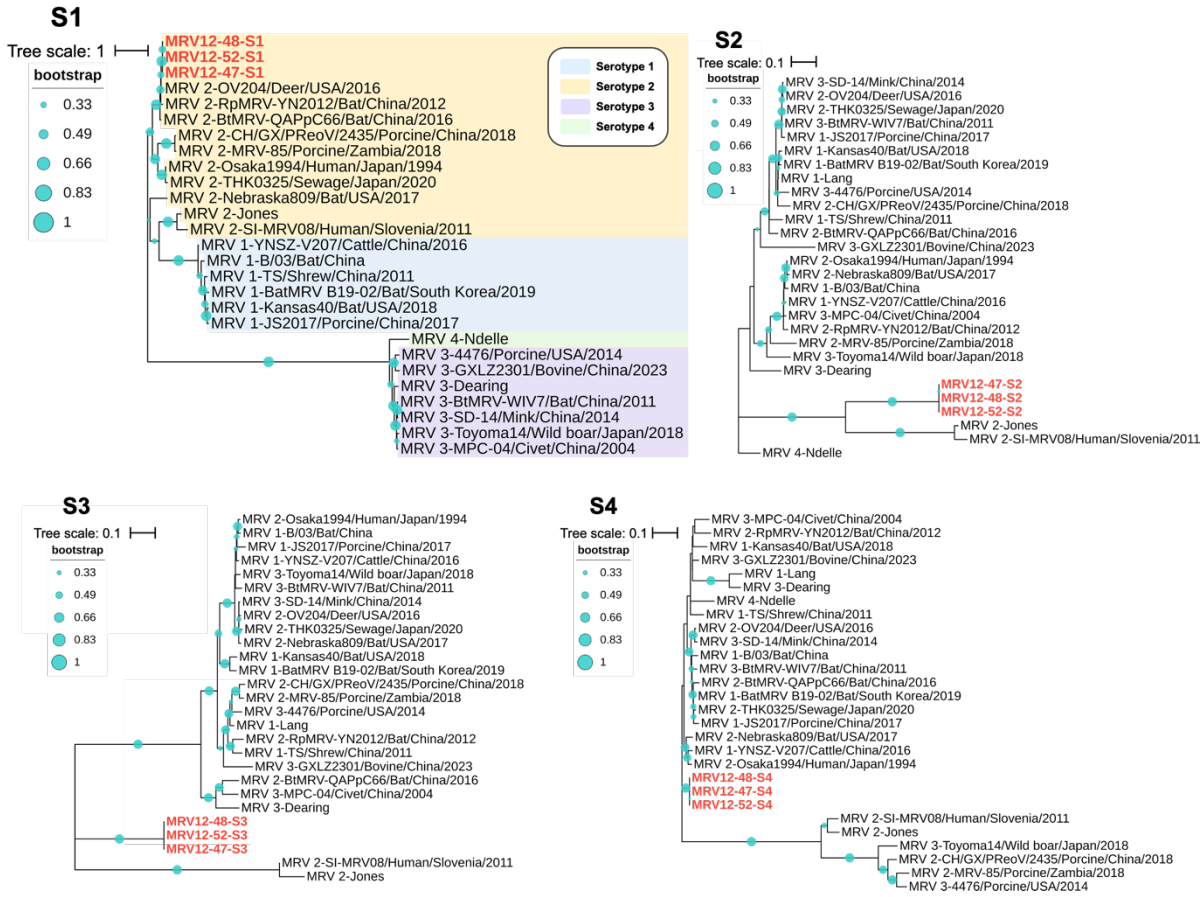

Figure 12. Phylogenetic tree of small (S) segments of the isolated MRVs. Coding nucleotide sequences of S1, S2, S3, and S4 segments of MRV12-47, MRV12-48, and MRV12-52 were aligned with the reference MRVs. Phylogenetic trees of each segment were constructed using the ML method with bootstrap values of 1,000 replicates. Serotypes of the MRVs were assigned based on the phylogenetic tree of the S1 segment. Serotypes 1, 2, 3, and 4 were highlighted in blue, yellow, purple and green colors, respectively.

(A)

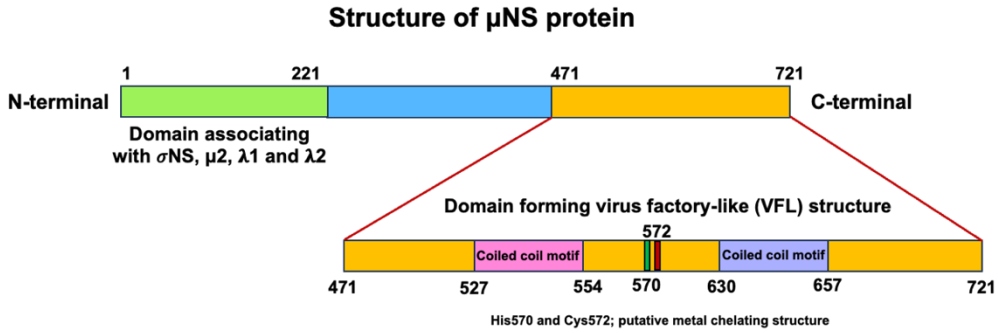

(B)

```
                 470        480        490        500        510        520        530        540        550
Consensus        LFLERXNDMVDGIKLQLDASRQCHECPVLQQKVVELEKQIIMQKSIQSDPTPMALQPLLSQLRELSSEVTRLQMELSRAQSLNAQLEADVKSA  558
Bat/MRV12-52     .YS.K...T.....................IA.....L.V.R.F.T.T.............................I.......M...  558
Type 1 Lang      ......S.....................................................................T..........A...  558
Type 2 Jones     ..MSS.S.T.................L....I.....HL.V...AS.....V.....................D...T.AI.TR........  558
Type 3 Dearing   ........VT.....................................V.....................................  558
Human/SI-MRV08   ..MSS.S.T.................L....I.....HM.V...TS.....V.....................T.AI.TR........  557
Pig/4476         .LP.....V............H.................V.....................................  558
Pig/CH/Gx/PReo   .LS.....V............H.................V.....................................  558
Bat/Kansas40     ...D.....................................V............T............G.I.....  558
Bat/YN2012       ...........................................................G.....................  558
Mink/SD-14       ...D.....................................................G.....................  558
Deer/OV204       ...D.....................................................G.....................  558

                  560        570        580        590        600        610        620        630        640        650
Consensus        QSCSLDMYLRHHTCINGHAKEDELLDAVRVAPDVRREIMEKRSEVRKGWCERISKEXAAKCQTVIDDLTLMNGKQAREITELRESAENYEKQI  651
Bat/MRV12-52     .A.............I.V...........SL...KD.LK..ET..QE.WD..A...SD.FSNQMEE..V...R..Q..AT...AVDT....V  651
Type 1 Lang      .A..............T.............K......G...R.....................Q.....................  651
Type 2 Jones     .........K......S.V.....M....I.....Q.L.L..KAT.QE.W...AR..STTF.SK..E.........H..S...D.VT.....V  651
Type 3 Dearing   ..........................................Q.....................Q......D...K.....  651
Human/SI-MRV08   ..............S.................Q.L.L..KAT.QE.W...A...STTF.SK..E.........H..S...D.VT.....V  650
Pig/4476         ....................................Q...R.............S.E......E.........Q..I...D.........  651
Pig/CH/Gx/PReo   ................V.....................R.............S.....M..E.........Q..I...D.........  651
Bat/Kansas40     ..........................................................R.........Q.....................  651
Bat/YN2012       ..........................I.........................R.......A......Q.....................  651
Mink/SD-14       ..........................................................HT........V.....................  651
Deer/OV204       ..........................I.....................................Q.....................  651

                         660        670        680        690        700        710        720
Consensus        AELVSTITQNQITYQQELQALVAKNVELDTLNQRQAKSLRITPSLLSATPIDSVDGAADLIDFSVPTDEL                      721
Bat/MRV12-52     S...N......V.............L...A......R.M.............T...PQNTT....SP...                      721
Type 1 Lang      ....G......M.................M.....................................                      721
Type 2 Jones     ...........T.............I...A........V...S.........A....S........A...                      721
Type 3 Dearing   ............................A.....................A..V.............                      721
Human/SI-MRV08   ....N......K.............I.............V...S.........A....S.......AA...                      720
Pig/4476         ..................................R..........V..T...................                      721
Pig/CH/Gx/PReo   ..................................R..........V..T...................                      721
Bat/Kansas40     ............................A.....................I...T.............                      721
Bat/YN2012       ..........................................................T.............                      721
Mink/SD-14       ..........................................................ST............                      721
Deer/OV204       ..........................................................SN............                      721
```

Figure 13. Multiple amino acid sequence alignment of viral μNS protein. (A) A schematic representation of μNS protein encoded by M3 segment of MRV. (B) Multiple comparisons of the 250 amino acids at the C-terminal of μNS. Amino acid sequences of μNS of MRV12-52 and the other related strains were aligned using Clustal omega. The unique amino acids of MRV12-52 were highlighted in red color.

Growth efficiency of MRV12-52 in cell lines

The growth efficiency of MRV12-52 in Vero E6, BHK-21, A549, Caco-2, and HEK293T cells which were inoculated at an MOI=0.01 were examined, and the viral titers in culture supernatants were quantified by FFA. In BHK-21, the titers of MRV12-52 were over 10^5 ffu/ml at 24 hpi and reached to 10^7 ffu/ml at 72 hpi (Figure 14A). HEK293T and A549 cells also supported the efficient proliferation of MRV12-52, while Vero E6 and Caco-2 cells were relatively less permissive to infection (Figure 14A). IFA staining of MRV12-52 antigens in each cell line at 48 hpi illustrated abundant viral antigens in BHK-21, HEK293T, and A549 cells (Figure 14B), supporting the results of growth curve analysis.

In this study, bat MRV was isolated using Vero T2-hACE2 cells. To investigate the impact of TMPRSS2- and ACE2-expressions on MRV infection, the growth efficiency of MRV12-52 was compared in Vero E6, Vero T2, and Vero T2-hACE2. The titers of MRV12-52 in Vero E6, Vero T2, and Vero T2-hACE2 were not significantly different at all time points (Figure 14C), indicating that the expression of TMPRSS2 and ACE2 in Vero cells did not enhance the growth of MRV12-52.

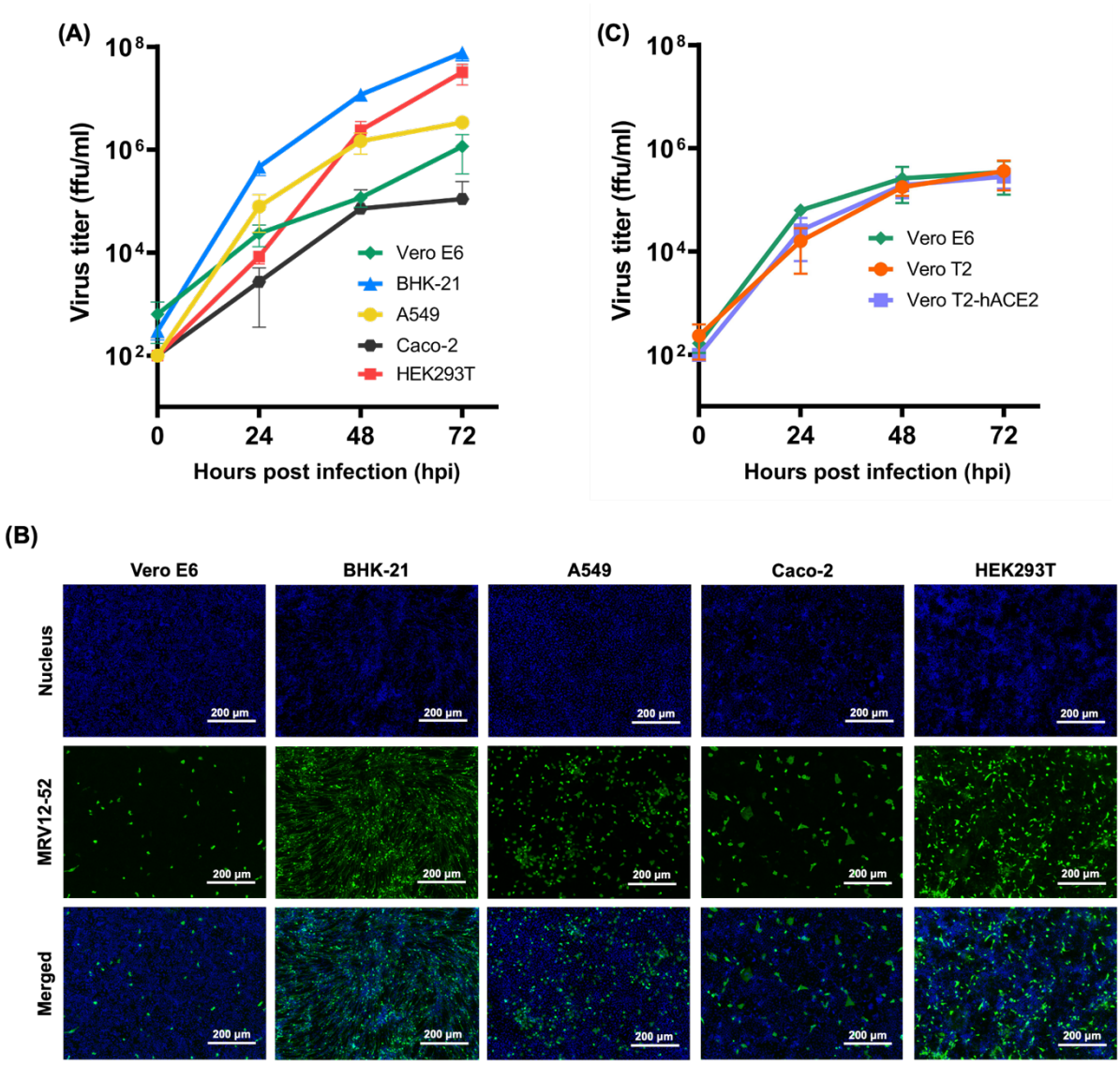

Figure 14. Growth efficiency of MRV12-52 in cell lines. (A) Growth kinetics of MRV12-52 in Vero E6, BHK-21, A549, Caco-2, and HEK293T cells. (B) IFA staining of MRV12-52 in cell lines. Cells were inoculated with MRV12-52 at an MOI=0.01 and fixed at 48 hpi. Cells were stained with anti-MRV12-52 polyclonal antibody for virus antigens (green) and Hoechst 33342 for cell nuclei (blue). Scale bars =200 μm. (C) Impact of exogenous expression of human TMPRSS2 and ACE2 on the growth kinetics of MRV12-52 in Vero E6 cells. Vero E6, Vero T2, and Vero T2-hACE2 cells were inoculated with MRV12-52 at an MOI of 0.01. Virus titers in the culture supernatants at 0, 24, 48, and 72 hpi were examined by FFA.

Experimental infection of laboratory mice with MRV12-52

To investigate the infectivity and pathogenicity of MRV12-52, viral loads, pathological changes, and survival rates of BALB/c mice inoculated with MRV12-52 were examined (Figure 15A). After inoculation with MRV12-52, mice increased their BW similar to PBS-inoculated mice. MRV12-52 inoculated mice showed BW decreases from 6 to 7 dpi (Figure 15B). Six out of eight mice (75%) developed severe body weight loss and reached the endpoint at 7 or 8 dpi. Two mice (25%) slightly decreased their BW at 7 dpi but recovered from the infection. Survival analysis demonstrated 75% mortality rate caused by MRV12-52 in mice (Figure 15C).

Next, the replication of MRV12-52 was examined in primary organs, including lung, liver, spleen, kidney, and intestine of mice. The viral titer in the lungs was significantly increased at 3 dpi and reached a peak at 5 dpi, thereafter the titer slightly declined at 7 dpi (Figure 15D). The virus titer was also detected in the intestine at 1 dpi and then diminished at 3, 5, and 7 dpi. However, the titers in the liver, spleen, and kidney were below the limits of detection indicating that MRV12-52 replicated primarily in the lung and intestine (Figure 15D). Consistently, RNA of the viral L2 gene was abundant in the lung at 3 dpi and decreased at 5 and 7 dpi (Figure 15E).

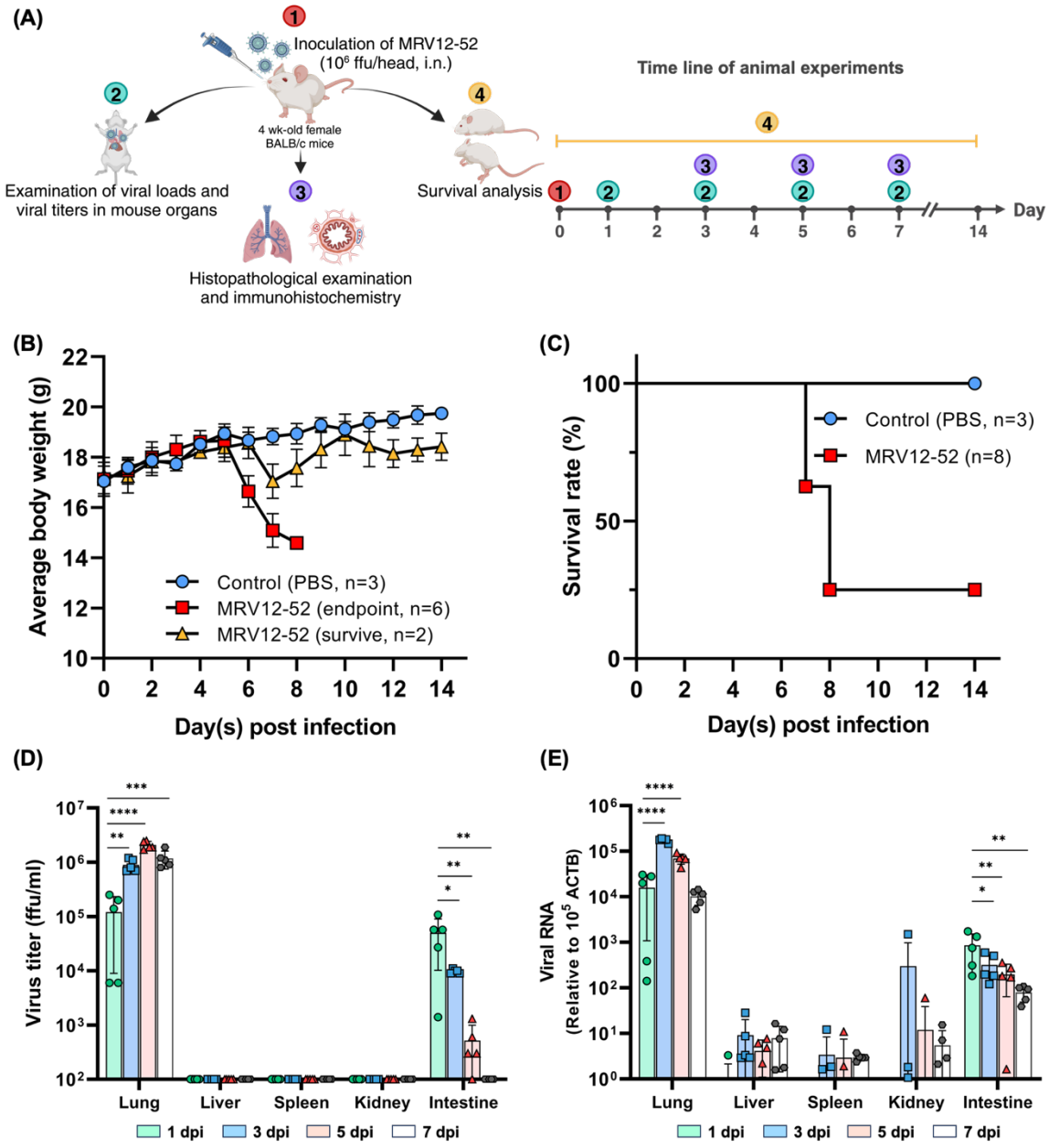

Figure 15. Replication and pathogenicity of MRV12-52 in laboratory mice. (A) Schematic overview of the experimental methods. Female BALB/c mice (4-week-old) were intranasally inoculated with 10^6 ffu of MRV12-52 or PBS as control. BW monitoring and organ collection were performed at each time points as indicated. Graphical illustration of animal experiment of MRV12-52 was made in BioRender.com. (B) BW change during the course of infection. (C) Kaplan-Meier survival analysis of mice infected with MRV12-52. A humane endpoint was considered when the mice showed more than 20% body weight loss. (D) Virus titers in the lung, liver, spleen, kidney, and intestine of mice at the indicated time points. (E) Viral RNA levels in organs of MRV12-52 inoculated mice. Data were normalized to the mRNA levels of mouse

ACTB and the relative expression of the L2 gene was calculated by the $2^{-\Delta Ct}$ method. One-way ANOVA with Dunnett's multiple comparisons was used to determine the statistical significance of differences in viral titers and viral RNA levels between 1 dpi, 3 dpi, 5 dpi and 7 dpi. *, $p < 0.01$; **, $p < 0.001$, ***, $p < 0.0002$; ****, $p < 0.0001$.

Lung pathology of MRV12-52-infected mice

To evaluate pathological changes caused by MRV12-52 infection, mice were sacrificed at 3, 5, and 7 dpi (Figure 15A). Hyperemia with edema were mainly observed at the right middle and inferior lobes of the lung of mice at 3 dpi. Lung pathology was shown to progress at 5 dpi and became more severe at 7 dpi with edema throughout the lungs (Figure 16A). Microscopic examination of the lung sections at 3, 5, and 7 dpi demonstrated diffuse inflammatory cell infiltration in the peribronchovascular area and alveolar space. Lymphocytic infiltration, interstitial pneumonia, and alveolar thickening were found in the lung at 5 and 7 dpi (Figure 16B), concordantly with the gross appearance of MRV12-52 infected lungs (Figure 16A). To detect viral antigens by IHC, anti-MRV12-52 polyclonal antibody was prepared by immunization of guinea pigs with MRV12-52. IHC detection demonstrated that MRV12-52 antigen was found abundantly in alveolar epithelial cells at 3 and 5 dpi but was limited at 7 dpi (Figure 16C). Furthermore, inflammatory cells were examined in the lung of MRV12-52 inoculated mice at 7 dpi by IHC with anti-CD3 antibody for T lymphocytes, anti-Iba1 antibody for macrophages, and anti-MPO antibody for neutrophils. Iba1-positve macrophages were the major immune cells seen in the responses to MRV12-52 infection. T lymphocytes were also found diffusely distributed in the alveolar space, while neutrophils were rarely detected (Figure 16D).

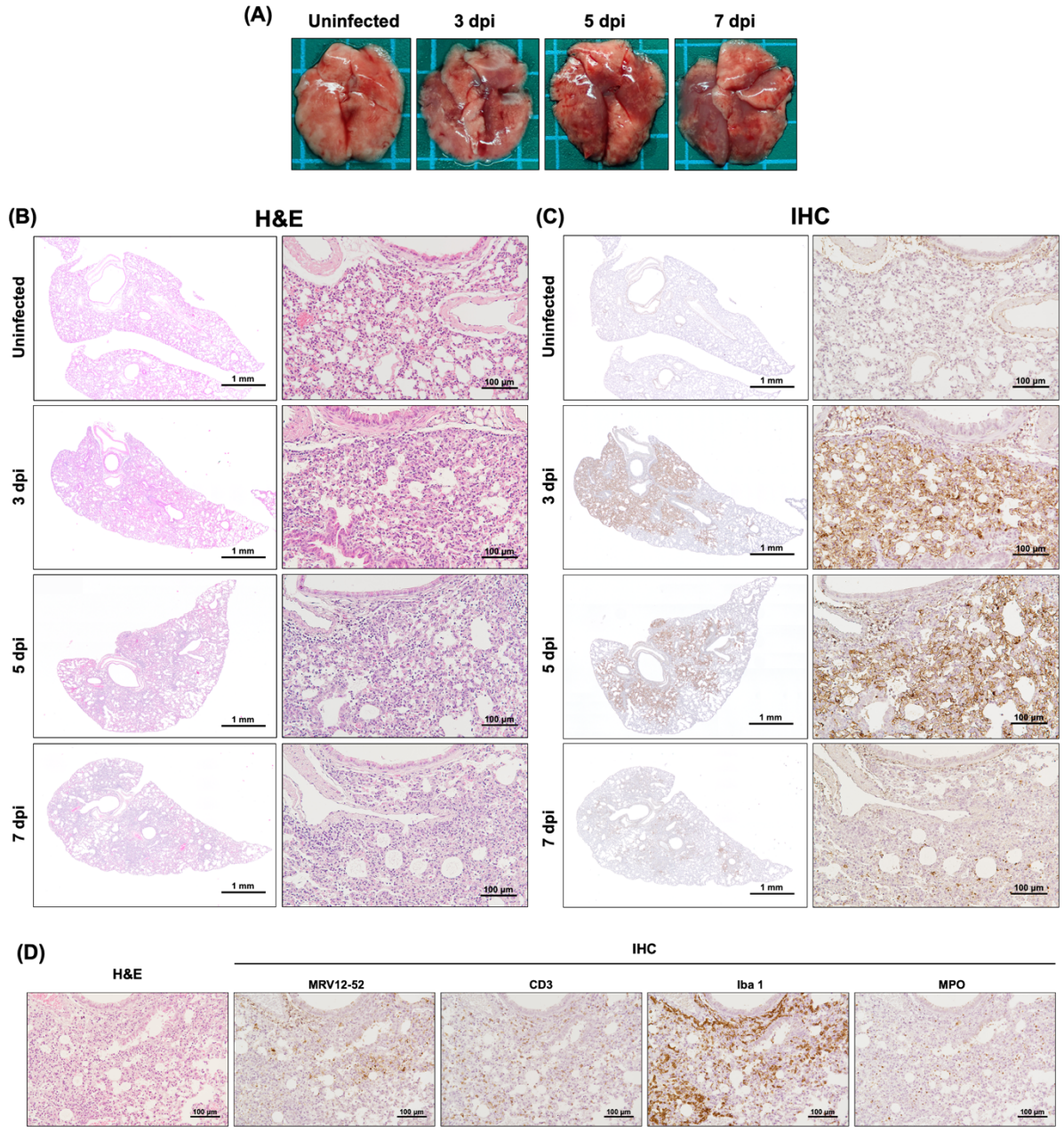

Figure 16. Pathological changes in the lungs of MRV12-52 infected mice. Lungs were collected from mice at 3, 5, and 7 dpi of MRV12-52 for the pathological examination. (A) Gross appearance of the lungs of mice inoculated with MRV12-52 or control PBS. (B) Histopathological images of the lung section by H&E staining. (C) Detection of MRV12-52 antigen in the lungs by IHC. Lung sections were stained with anti-MRV12-52 polyclonal antibody and counterstained for cell nuclei with Hematoxylin. (D) H&E staining and IHC on serial sections of the lung at 7 dpi. For IHC, the sections were stained for MRV12-52, CD3 for T lymphocytes, Iba1 for macrophages, and MPO for neutrophils. Scale bars in each image was indicated as 1 millimeter (mm) or 100 μm.

Discussion

The emergence of bat ORVs has become a public health concern in the past few decades. Several bat ORVs belonging to NBV species, including KamV, MelV, Sikamat, Miyazaki-Bali/2007, HK/07, HK/09, and HK/10 have been reported to cause acute respiratory tract infections in humans, especially in Malaysia and Indonesia, indicating the emergence of ORV spillover from bats to humans in SEA[23-27]. Previously, NBV, named PgORV from fruit bats in Indonesia was isolated[90]. Other ORV species, MRV, have been widely reported from livestock, bats, wildlife, humans, and environmental samples in many countries and regions, including China, Japan, Korea, Taiwan, Europe, Africa, and America[10-13, 28-40, 75-83, 87-89]. However, there have been no reports on MRV in bats, wildlife, livestock or humans in the SEA region, while NBV has been detected sporadically in fruit bats and humans in several SEA countries, including Malaysia, Indonesia, and the Philippines[17, 20-27]. In the current study, three MRV isolates, MRV12-47, MRV12-48, and MRV12-52 were isolated from IFBs. This study is the first report of isolation and characterization of MRV in the SEA region.

Fruit bats belonging to the family *Pteropodidae* serve as natural reservoirs of NBV[15, 17-18, 90]. In contrast, most MRVs have been identified and isolated from various species of insectivorous bats including, *Rhinolophus spp.*, *Myotis spp.*, *Hipposideros spp.*, *Pipistrellus spp.*, *Vespertilio spp.*, *Eptesicus spp.*, *Lasiurus spp.,* and *Lasionycteris spp.*, suggesting that insectivorous bats may play an important role as a main reservoir of bat MRVs[10-13, 29-34]. In this study, MRVs were isolated from fecal samples of large flying foxes (*P. vampyrus*). Moreover, another study has reported MRV isolated from short-nosed fruit bats (*Cynopterus sphinx*) in China[28]. These findings indicated that fruit bats as well as insectivorous bats can harbor MRVs.

Genes encoding core proteins, including L1-L3, M1, M3, S2, and S3 were highly conserved among MRVs with more than 85% of nucleotide sequence identity [11, 13, 29, 75-76, 78, 80-82]. Conversely, pairwise comparison of L1-L3, M1-M3, S2, and S3 segments of MRV12-52 displayed low nucleotide sequence identities ranging from 73.3 to 80.8% to the closest MRV strains. Moreover, phylogenetic analysis of these segments displayed the unique lineage of MRV12-52 that was evolutionary distinct from the known MRV strains. Multiple sequence alignment of the representative core protein, μNS showed significant amino acid sequence differences between MRV12-52 and the prototype MRV strains at positions 471 to 721, where is the domain associated with VFL formation in MRV-infected cells. These data highlighted the unique genetic background of MRV12-52, the first MRV isolated from fruit bats in

Indonesia. Because of MRVs have high diversity in their genome segments, the recent study on MRV genome constellations proposed that the genotypes of MRVs can be assigned to each segment and the minimum intragenotype sequence identities of each segment range from 77-88%[94]. According to the data in this study, L2, M1, and M3 segments displayed sequence identities of 75.7, 73.3, and 74.8%, respectively, suggesting that these segments of MRV12-52 may form unique genotypes from the other MRV strains. However, these data are not sufficient to conclude whether such unique genome characteristics will be found in the other animals and humans in SEA. Continuing studies of genetic evolutions in bats, wildlife, livestock, and humans will bridge the gap of knowledge and provide more information on the circulation and distribution of MRV in the SEA region.

Reassortments were evident in several MRV strains[13, 29, 81, 87-88]. In the present study, S1 and S4 segments of MRV12-47, MRV12-48, and MRV12-52 had high sequence identities with those of MRVs from deer (93.6%) and humans (95.3%), respectively. Phylogenetic analysis revealed that MRV12-47, MRV12-48, and MRV12-52 formed a cluster with known MRVs in the trees of the S1 and S4 segments but were segregated in the trees of L1, L2, L3, M1, M2, M3, S2, and S3 segments. These incongruences suggest past reassortment event(s) between the MRV12-47, MRV12-48, and MRV12-52 genomes and the other strains identified from deer and humans, implying cross-species transmission in bats, wildlife, and humans.

In the previous study by Anindita *et al*., a betacoronavirus genome was detected in a Moluccan naked-backed fruit bat (*D. moluccensis*) collected in Paguyaman in 2012[52]. Virus isolation was attempted using several cell lines, including bat-derived cell lines, but failed to recover any coronavirus from coronavirus-positive fecal samples. At the beginning of this study, sarbecovirus and other betacoronaviruses were targeted for isolation from IFBs. While sarbecovirus was successfully isolated from *Rhinolophus cornutus* using cells expressing TMPRSS2 and ACE2 of *R. cornutus*, this indicated that the virus had a narrow host range and might be specific to bat species[95]. In this study, cells co-expressing TMPRSS2 and ACE2 of *D. moluccensis* and *A. celebensis* were generated and employed to facilitate sarbecovirus isolation. Unfortunately, no coronaviruses were isolated using this approach. Since the partial genome of the coronavirus detected in IFBs was assigned to the nobecovirus lineage, it is possible that the virus may not use ACE2 as a receptor for cell entry.

In the present study, the properties and pathogenicity of MRV12-52 was evaluated by virus inoculation into BALB/c mice. The result demonstrated that MRV12-52 replicated

efficiently in the lung and caused severe respiratory diseases in laboratory mice with a high mortality of up to 75%. Other studies by Jiang, Do, and Li *et al*. also showed that intranasal inoculation of mice with MRVs isolated from bats resulted in BW loss and respiratory distress; however, the mortality rates varied from 0-50% depending on the virus strains and infectious doses[28, 31, 96]. The respiratory tract and gastrointestinal tract are the main targets of MRV12-52 replication. The virus did not disseminate to other organs such as the liver, spleen, or kidney. In contrast, WIV2, WIV3, and WIV7 strains isolated from insectivorous bats and the B/03 strain isolated from wild short-nosed fruit bats in China exhibited systemic infection involving the intestine, liver, spleen, brain, heart, and kidney [28, 96], supporting the view that the infectivity and pathogenicity of MRV may depend on the virus strain. To assess the burden and zoonotic potential of the isolated MRVs, further epidemiological and virological studies should be performed in bat populations and humans in Indonesia.

In conclusion, MRVs from large flying foxes in Indonesia were isolated and this is the first report of MRV in the SEA region. Characterization of the isolated MRV (MRV12-52) suggested a unique evolutional history and the possible previous reassortment of S1 and S4 segments with other MRVs. It is also demonstrated that MRV12-52 causes lethal infection with severe pneumonia in laboratory mice. In future studies, knowledge on virus characteristics, infectivity, and pathogenicity will highlight the importance of MRV as a potential public health threat. Virus surveillance in bats, wildlife, domestic animals, and humans are now needed to be continued to better understand the evolution, distribution, transmission, and the zoonotic potential of bat MRV in Indonesia and the SEA region.

General conclusion

Research on bat-borne viruses has significantly intensified in recent years due to their role in several high-profile zoonotic outbreaks. Advances in genomic sequencing have allowed researchers to identify a vast array of viruses in bat populations worldwide. This ongoing discovery process is crucial for understanding the genetic diversity of these viruses and their potential for zoonotic transmission. However, most studies have focused on identifying virus sequences rather than characterizing their functions or the ecological and epidemiological factors facilitating spillover.

To gain a holistic view in the study of bat-borne viruses, integrative studies using various approaches are required. Advanced methods, such as HTS have revolutionized bat-borne virus research by enabling the rapid and comprehensive sequencing of viral genomes directly from bat samples. This allows researchers to discover new viruses, study their genetic diversity, and track their evolution. Meanwhile, traditional methods can provide the fundamental data needed to identify and characterize viruses. Furthermore, integrating ecological data with genomic insights helps to create a comprehensive understanding of how viruses circulate within bat populations and spill over to other species.

In chapter I, a new member of the NBV species (PgORV) was isolated from fecal samples of IFBs collected in Paguyaman, North Sulawesi, Indonesia, in 2013. Molecular characterization revealed past reassortment events with zoonotic strains MB/07 and Sikamat, isolated from patients, respectively, in Indonesia and Malaysia, and bat strains (Samal-24 and Talikud-80) isolated in Philippines. PgORV well replicated in human-derived cell lines, and inoculation of PgORV into laboratory mice demonstrated severe pneumonia in the mice, indicating its potential pathogenicity in mammals. Additionally, serosurveillance of NBVs displayed high prevalence in IFBs, indicating the risk of disease transmission from bats to other animals and humans.

In chapter II, a new virus belonging to MRV was isolated from IFBs using an cultured cell-based approach and its genome and virological properties were characterized. The isolated MRV (MRV12-52) possessed a unique genetic background distinct from other known MRV strains isolated from bats, domestic animals, wildlife, humans, and environmental samples. While MRVs typically cause asymptomatic or mild gastrointestinal infections, MRV12-52 caused severe pneumonia in laboratory mice with a high mortality rate of 75%. This study highlights the significance of bat-borne MRV in Indonesia as a possible public health threat.

This dissertation exemplifies the integrative study of bat-borne viruses. Despite the extensive information already available on viruses carried by bats, it still important to understand and mitigate the risks associated with bat-borne viruses, ultimately contributing to global health security to prevent future outbreaks posed by bats.

Acknowledgment

I would like to express my sincere gratitude to my supervisors, Prof. Hirofumi Sawa, Prof. Yasuko Orba and Assoc. Prof. Michihito Sasaki for their constant support and guidance in my studies. I would like to especially thank Prof. Sawa and Dr. Sasaki for his kind effort, patience, and mentorship in training me in the laboratory procedures in my bat-borne virus research.

My deepest gratitude also goes to Prof. Hiroaki Kariwa, Laboratory of Public Health, Department of Preventive Veterinary Medicine, Graduate School of Veterinary Medicine, Assoc. Prof. Keita Matsuno, Division of Risk Analysis, International Institute for Zoonosis Control, for constructive comments and suggestions on my research, Prof. Agus Setiyono and Prof. Egowati Handharyani, Department of Veterinary Clinic, Reproduction and Pathology, Faculty of Veterinary Medicine, IPB University, Bogor, Indonesia, for their kind support on bat research in Indonesia. Prof. William W. Hall, Prof. Takashi Kimura, Dr. Masayuki Saijo, Dr. Satoshi Taniguchi, Dr. Hayato Harima for their support and guidance on my research.

I would like to thank Specially appointed Ass. Prof. Koshiro Tabata and Specially appointed Ass. Prof. Yukari Itakura, my lovely senior and my best friend in Japan for their positive vibes, guidance, warm support, and encouragement.

I would like to thank Assoc. Prof. Masahiro Kajihara, Specially appointed Ass. Prof. Naganori Nao, Prof. Kimitake Funakoshi, Assoc. Prof. Kuniko Kawai, Ass. Prof. Kosuke Okuya, Dr. Katendi Changula, Ass. Prof. Shohei Ogata, Specially appointed Ass. Prof. Misheck Shawa, Dr. Joseph, and all staff in Zambia for their kind support on my bat activities in Japan and Zambia. I have learned many things about bats and gained invaluable field experiences related to bats from them.

I thank my laboratory colleagues; Dr. Uemura, Dr. Herman, Dr. Kishimoto, Hiroko Kobayashi, Takuma Ariizumi, Nijiho Kawaguchi, Kurouji-san, Fujikawa-san, Shionogi members; Dr. Sato, Dr. Kusakabe, Dr. Toba, Konishi-san, Hayashi-san, and IIZC and WISE staff for their continuing support and encouragement throughout my studies.

I am deeply thank to my family for their love and support in every step of my life, my 2 lovely daughters (cats) for their magic power that always recharge my life battery, and my friends, especially Fai, Ek, Yam, Chompoo, Great, Tiew, Ploy, Tong, Mon, Jib, Yannick, Hiroko, Ari, and Nijiho for friendship, encouragement, and mental support.

Finally, I am deeply thanks to the Ministry of Education, Culture, Sports, Science and Technology, Japan for the scholarship throughout the PhD course, and the Hokkaido University WISE program for One Health Frontier for the financial support of my academic activities. I greatly appreciated their support on my PhD.

References

1. Morse SS. Factors in the Emergence of Infectious Diseases. *Emerg Infect Dis* **1(1)**, 7-15 (1995).
2. Johns Hopkins Bloomberg School of Public Health. 2024. Difining Disease X. https://publichealth.jhu.edu/2024/what-is-disease-x [accessed on May 10, 2024].
3. Wong S, Lau S, Woo P, *et al*. Bats as a continuing source of emerging infections in humans. *Rev Med Virol* **17(2)**, 67-91 (2007).
4. Han HJ, Wen HL, Zhou CM, *et al*. Bats as reservoirs of severe emerging infectious diseases. *Virus Res* **205**, 1-6 (2015).
5. Letko M, Seifert SN, Olival KJ, *et al.* Bat-borne virus diversity, spillover and emergence. *Nat Rev Microbiol* **18**, 461–471 (2020).
6. Lau SKP, Luk HKH, Wong ACP, *et al*. Possible bat origin of severe acute respiratory syndrome coronavirus 2. *Emerg Infect Dis* **26(7)**, 1542-1547 (2020).
7. Voskarides, K. SARS-CoV-2: tracing the origin, tracking the evolution. *BMC Med Genomics* **15**, 62 (2022).
8. Wacharapluesadee S, Tan CW, Maneeorn P. *et al.* Evidence for SARS-CoV-2 related coronaviruses circulating in bats and pangolins in Southeast Asia. *Nat Commun* **12**, 972 (2021).
9. Gard G, Compans RW. Structure and cytopathic effects of Nelson Bay Virus. *J Virol* **6(1)**, 100-6 (1970).
10. Lelli D, Moreno A, Lavazza A, *et al.* Identification of mammalian orthoreovirus type 3 in Italian bats. *Zoonoses Public Health* **60(1)**, 84–92 (2013).
11. Wang L, Fu S, Cao L, *et al.* Isolation and identification of a natural reassortant mammalian orthoreovirus from Least horseshoe bat in China. *PLoS One* **10(3)**, e0118598 (2015).
12. Kohl C, Lesnik R, Brinkmann A, *et al.* Isolation and characterization of three mammalian orthoreoviruses from European bats. *PLoS One* **7(8)**, e43106 (2012).
13. Naglič T, Rihtarič D, Hostnik P, *et al.* Identification of novel reassortant mammalian orthoreoviruses from bats in Slovenia. *BMC Vet Res* **14**, 264 (2018).
14. Du L, Lu Z, Fan Y, *et al.* Xi River virus, a new bat reovirus isolated in southern China. *Arch Virol* **155(8)**, 1295-9 (2010).
15. Bennett AJ, Goldberg TL. Pteropine orthoreovirus in an Angolan soft-furred fruit bat (*Lissonycteris angolensis*) in Uganda dramatically expands the global distribution of an emerging bat-borne respiratory virus. *Viruses* **12(7)**, 740 (2020).
16. Thalmann CM, Cummins DM, Yu M, *et al.* Broome virus, a new fusogenic orthoreovirus species isolated from an Australian fruit bat. *Virology* **402(1)**, 26–40 (2010).
17. Taniguchi S, Maeda K, Horimoto T, *et al.* First isolation and characterization of pteropine orthoreoviruses in fruit bats in the Philippines. *Arch Virol* **162(6)**, 1529–1539 (2017).

18. Harima H, Sasaki M, Orba Y, *et al.* Attenuated infection by a pteropine orthoreovirus isolated from an Egyptian fruit bat in Zambia. *PLoS Negl Trop Dis* **15(9)**, e0009768 (2021).

19. Hu T, Qiu W, He B, *et al.* Characterization of a novel orthoreovirus isolated from fruit bat, China. *BMC Microbiol* **14**, 293 (2014).

20. Lorusso A, Teodori L, Leone A, *et al.* A new member of the pteropine orthoreovirus species isolated from fruit bats imported to Italy. *Infect Genet Evol* **30**, 55–58 (2015).

21. Pritchard LI, Chua KB, Cummins D, *et al.* Pulau virus; a new member of the Nelson Bay orthoreovirus species isolated from fruit bats in Malaysia. *Arch Virol* **151(2)**, 229–39 (2006).

22. Takemae H, Basri C, Mayasari NLPI, *et al.* Isolation of pteropine orthoreovirus from *Pteropus vampyrus* in Garut, Indonesia. *Virus Genes* **54(6)**, 823–827 (2018).

23. Chua KB, Voon K, Yu M, *et al.* Investigation of a potential zoonotic transmission of orthoreovirus associated with acute influenza-like illness in an adult patient. *PLoS One* **6(10)**, e25434 (2011).

24. Yamanaka A, Iwakiri A, Yoshikawa T, *et al.* Imported case of acute respiratory tract infection associated with a member of species nelson bay orthoreovirus. *PLoS One* **9(3)**, e92777 (2014).

25. Wong AH, Cheng PKC, Lai MYY, *et al.* Virulence potential of fusogenic orthoreoviruses. *Emerg Infect Dis* **18(6)**, 944-8 (2012).

26. Chua KB, Voon K, Crameri G, *et al.* Identification and characterization of a new orthoreovirus from patients with acute respiratory infections. *PLoS One* **3(11)**, e3803 (2008).

27. Chua KB, Crameri G, Hyatt A, *et al.* A previously unknown reovirus of bat origin is associated with an acute respiratory disease in humans. *Proc Nalt Acad Sci USA* **104(27)**, 11424-11429 (2007).

28. Li Z, Liu D, Ran X, Liu C, Guo D, *et al.* Characterization and pathogenicity of a novel mammalian orthoreovirus from wild short-nosed fruit bats. *Infect Genet Evol* **43**, 347–53 (2016).

29. Yan X, Sheng J, Zhang C, *et al.* Detection and characterization of a reassortant mammalian orthoreovirus isolated from bats in Xinjiang, China. *Viruses* **14(9)**, 1897 (2022).

30. Wang L, Zheng B, Shen Z, *et al.* Isolation and characterization of mammalian orthoreovirus from bats in the United States. *J Med Virol* **95(2)**, e28492 (2023).

31. Do HQ, Yeom M, Moon S, *et al*. Genetic characterization and pathogenicity in a mouse model of newly isolated bat-originated mammalian orthoreovirus in South Korea. *Microbiol Spectr* **12**, e01762-23 (2024).

32. Ichikawa A, Katayama M, Lai H, *et al.* Isolation and genetic characterization of a mammalian orthoreovirus from *Vespertilio sinensis* in Japan. *Arch Virol* **168(6)**, 165 (2023).

33. Lo VT, Yoon SW, Noh JY, *et al.* Characterization of replication and variations in genome segments of a bat reovirus, Bat MRV/B19-02, by RNA-seq in infected Vero-E6 cells. *Arch Virol* **167(11)**, 2133–2142 (2022).

34. Feng KH, Brown JD, Turner GG, *et al*. Unrecognized diversity of mammalian orthoreoviruses in North American bats. *Virology* **571**, 1–11 (2022).

35. Steyer A, Gutiérrez-Aguire I, Kolenc M, *et al.* High similarity of novel orthoreovirus detected in A child hospitalized with acute gastroenteritis to mammalian orthoreoviruses found in bats in Europe. *J Clin Microbiol* **51(11)**, 3818–25 (2013).

36. Rosa UA, Ribeiro G de O, Villanova F, *et al.* First identification of mammalian orthoreovirus type 3 by gut virome analysis in diarrheic child in Brazil. *Sci Rep* **9(1)**, 18599 (2019).

37. Yamamoto SP, Motooka D, Egawa K, *et al.* Novel human reovirus isolated from children and its long-term circulation with reassortments. *Sci Rep* **10**, 963 (2020).

38. Tyler KL, Barton ES, Ibach ML, *et al.* Isolation and molecular characterization of a novel type 3 reovirus from a child with meningitis. *J Infect Dis* **189(9)**, 1664-75 (2004).

39. Ouattara LA, Barin F, Barthez MA, *et al.* Novel human reovirus isolated from children with acute necrotizing encephalopathy. *Emerg Infect Dis* **17(8)**, 1436-44 (2011).

40. Richardson SC, Bishop RF, Smith AL. Reovirus serotype 3 infection in infants with extrahepatic biliary atresia or neonatal hepatitis. *J Gastroenterol Hepatol* **9(3)**, 264-8 (1994).

41. The International Committee on Taxonomy of Viruses (ICTV). 2024. Genus: Orthoreovirus. https://ictv.global/report/chapter/spinareoviridae/spinareoviridae/orthoreovirus [accessed on May 26, 2024].

42. Singh H, Shimojima M, Ngoc TC, *et al*. Serological evidence of human infection with Pteropine orthoreovirus in Central Vietnam. *J Med Virol* **87(12)**, 2145-8 (2015).

43. Leong WJ, Quek XF, Tan HY, *et al*. Seroprevalence of pteropine orthoreovirus in humans remain similar after nearly two decades (2001-2002 vs. 2017) in Tioman Island, Malaysia. *J Med Virol* **94(2)**, 771-775 (2022).

44. Uehara A, Tan CW, Mani S, *et al*. Serological evidence of human infection by bat orthoreovirus in Singapore. *J Med Virol* **91**, 707-710 (2019).

45. Tee KK, Chan PQ, Loh AM, *et al*. Surveillance, isolation and genomic characterization of pteropine orthoreovirus of probable bat origin among patients with acute respiratory infection in Malaysia. *J Med Virol* **95(2)**, e28520 (2023).

46. World population review. 2024. Bat population by country 2024. https://worldpopulationreview.com/country-rankings/bat-population-by-country [accessed on May 29, 2024].

47. Sasaki M, Setiyono A, Handharyani E, *et al.* Isolation and characterization of a novel alphaherpesvirus in fruit bats. *J Virol* **88(17)**, 9819–29 (2014).

48. Wada Y, Sasaki M, Setiyono A, *et al.* Detection of novel gammaherpesviruses from fruit bats in Indonesia. *J Med Microbiol* **67(3)**, 415–422 (2018).

49. Sendow I, Ratnawati A, Taylor T, *et al*. Nipah virus in the fruit bat *Pteropus vampyrus* in Sumatera, Indonesia. *PLoS One* **8(7)**, e69544 (2013).

50. Kobayashi S, Sasaki M, Nakao R, *et al.* Detection of novel polyomaviruses in fruit bats in Indonesia. *Arch Virol* **160(4)**, 1075–82 (2015).

51. Sasaki M, Gonzalez G, Wada Y, *et al.* Divergent bufavirus harboured in megabats represents a new lineage of parvoviruses. *Sci Rep* **6**, 24257 (2016).

52. Anindita PD, Sasaki M, Setiyono A, *et al.* Detection of coronavirus genomes in Moluccan naked-backed fruit bats in Indonesia. *Arch Virol* **160(4)**, 1113–8 (2015).

53. Sasaki M, Setiyono A, Handharyani E, *et al.* Molecular detection of a novel paramyxovirus in fruit bats from Indonesia. *Virol J* **9**, 240 (2012).

54. Sasaki M, Uemura K, Sato A *et al.* SARS-CoV-2 variants with mutations at the S1/S2 cleavage site are generated in vitro during propagation in TMPRSS2-deficient cells. *PLoS Pathog* **17(1)**, e1009233 (2021).

55. Wellehan JFX, Childress AL, Marschang RE, *et al.* Consensus nested PCR amplification and sequencing of diverse reptilian, avian, and mammalian orthoreoviruses. *Vet Microbiol* **133(1-2)**, 34–42 (2009).

56. Kumar S, Stecher G, Tamura K. MEGA7: Molecular evolutionary genetics analysis version 7.0 for bigger datasets. *Mol Biol Evol* **33(7)**, 1870–4 (2016).

57. Kanai Y, Kawagishi T, Sakai Y, *et al.* Cell-cell fusion induced by reovirus FAST proteins enhances replication and pathogenicity of non-enveloped dsRNA viruses. *PLoS Pathog* **15(4)**, e1007675 (2019).

58. Livak KJ, Schmittgen TD. Analysis of relative gene expression data using real-time quantitative PCR and the $2^{-\Delta\Delta CT}$ method. *Methods* **25(4)**, 402–8 (2001).

59. Kosoltanapiwat N, Reamtong O, Okabayashi T, *et al.* Mass spectrometry-based identification and whole-genome characterisation of the first pteropine orthoreovirus isolated from monkey faeces in Thailand. *BMC Microbiol* **18**, 135 (2018).

60. Kimprasit T, Nunome M, Iida K *et al.* Dispersal history of *Miniopterus fuliginosus* bats and their associated viruses in East Asia. *PLoS One* **16(1)**, e0244006 (2021).

61. Breed AC, Field HE, Smith CS, *et al*. Bats without borders: long-distance movements and implications for disease risk management. *EcoHealth* **7(2)**, 204–12 (2010).

62. Randhawa N, Bird BH, Van Wormer E *et al.* Fruit bats in flight: a look into the movements of the ecologically important *Eidolon helvum* in Tanzania. *One Health Outlook* **2**, 16 (2020).

63. Dermody TS, Parker JS, Sherry B. Fields Virology: Orthoreoviruses, 6th ed. Vol. 2. Wolters Kluwer/Lippincott Williams, & Winlkins, Philadelphia, United States, pp. 1304-1346 (2013).

64. Cifuentes- Muñoz N, Dutch RE, Cattaneo R. Direct cell-to-cell transmission of respiratory viruses: The fast lanes. *PLoS Pathog* **14(6)**, e1007015 (2018).

65. Marsh M, Helenius A. Virus Entry: Open Sesame. *Cell* **124(4)**, 729-40 (2006).

66. Zhong P, Agosto LM, Munro JB, *et al*. Cell-to-cell transmission of viruses. *Curr Opin Virol* **3(1)**, 44-50 (2013).

67. Tarigan R, Katta T, Takemae H, *et al*. Distinct interferon response in bat and other mammalian cell lines infected with pteropine orthoreovirus. *Virus Genes* **57(6)**, 510-520.

68. Egawa K, Shimojima M, Taniguchi S, *et al*. Virulence, pathology, and pathogenesis of pteropine orthoreovirus (PRV) in BALB/c mice: Development of an animal infection model for PRV. *PLoS Negl Trop Dis* **11(22)**, e0006076.

69. Kanai Y, Kawagishi T, Okamoto M, *et al*. Lethal murine infection model for human respiratory disease-associated pteropine orthoreovirus. *Virology* **514**, 57-65 (2018).

70. Myers MA, Smith AP, Lane LC, *et al.* Dynamically linking influenza virus infection kinetics, lung injury, inflammation, and disease severity. *eLife* **10**, e68864 (2021).

71. Ostler T, Davidson W, Ehl S. Virus clearance and immunopathology by $CD8^+$ T cells during infection with respiratory syncytial virus are mediated by IFN-γ. *Eur J Immunol* **32(8)**, 2117-23 (2002).

72. Winkler ES, Bailey AL, Kafai NM, *et al.* SARS-CoV-2 infection of human ACE2-transgenic mice causes severe lung inflammation and impaired function. *Nat Immunol* **21**, 1327–1335 (2020).

73. Morris DR, Ansar M, Qu Y, *et al.* Combined blockade of IFN-Type I and TNF alpha receptors provides protection against respiratory syncytial virus (RSV)-induced disease and bronchoconstriction. *J Immunol* **206(1_Supplement)**, 20.14 (2021).

74. Karki R, Sharma BR, Tuladhar S, *et al.* Synergism of TNF-α and IFN-γ triggers inflammatory cell death, tissue damage, and mortality in SARS-CoV-2 infection and cytokine shock syndromes. *Cell* **184(1)**, 149-168 (2021).

75. Harima H, Sasaki M, Kajihara M, *et al*. Characterization of mammalian orthoreoviruses isolated from faeces of pigs in Zambia. *J Gen Virol* **101(10)**, 1027-1036 (2020).

76. Zhang W, Kataoka M, Doan YH, *et al*. Isolation and characterization of mammalian orthoreovirus type 3 from fecal sample from a wild boar in Japan. *Arch Virol* **166(6)**, 1671-1680 (2021).

77. Narayanappa AT, Sooryanarain H, Deventhiran J, *et al*. A novel pathogenic mammalian orthoreovirus from diarrheic pigs and swine blood meal in the United States. *mBio* **6(3)**, 00593-15 (2015).

78. Yang DK, An S, Park Y, *et al*. Isolation and identification of mammalian orthoreovirus type 3 from a Korean roe deer (*Capreolus pygargus*). *Korean J Vet Res* **61(2)**, e13 (2021).

79. Li Z, Shao Y, Liu C, *et al*. Isolation and pathogenicity of the mammalian orthoreovirus MPC/04 from masked civet cats. *Infect Genet Evol* **36**, 55-61 (2015).

80. Yang XL, Tan B, Wang B, *et al.* Isolation and identification of bat viruses closely related to human, porcine and mink orthoreoviruses. *J Gen Virol* **96(12)**, 3525–3531 (2015).

81. Ahasan MS, Subramaniam K, Sayler KA, *et al.* Molecular characterization of a novel reassortment mammalian orthoreovirus type 2 isolated from a Florida white-tailed deer fawn. *Virus Res* **270**, 197642 (2019).

82. Kitamura K, Takagi H, Oka T, *et al.* Intertypic reassortment of mammalian orthoreovirus identified in wastewater in Japan. *Sci Rep* **11**, 12583 (2021)

83. Lim MCY, Wang YF, Huang SW, *et al.* High incidence of mammalian orthoreovirus identified by environmental surveillance in Taiwan. *PLoS One* **10(11)**, e0142745 (2015).

84. Dermody TS, Schiff LA, Nibert ML, *et al.* The S2 gene nucleotide sequences of prototype strains of the three reovirus serotypes: characterization of reovirus core protein sigma 2. *J Virol* **65(11)**, 5721-31 (1991).

85. Breun LA, Broering TJ, McCutcheon AM, *et al.* Mammalian reovirus L2 gene and λ2 core spike protein sequences and whole-genome comparisons of reoviruses type 1 Lang, type 2 Jones, and type 3 Dearing. *Virology* **287(2)**, 333–48 (2001).

86. Attoui H, Biagini P, Stirling J, *et al.* Sequence characterization of Ndelle virus genome segments 1, 5, 7, 8, and 10: Evidence for reassignment to the genus Orthoreovirus, family Reoviridae. *Biochem Biophys Res Commun* **287(2)**, 583–8 (2001).

87. Wang L, Li Y, Walsh T, *et al.* Isolation and characterization of novel reassortant mammalian orthoreovirus from pigs in the United States. *Emerg Microbes Infect* **10(1)**, 1137–1147 (2021).

88. Fukase Y, Minami F, Masuda T, *et al.* Genetic diversity, reassortment, and recombination of mammalian orthoreoviruses from Japanese porcine fecal samples. *Arch Virol* **167(12)**, 2643–2652 (2022).

89. Miyaoka Y, Kadota C, Kabir MH, *et al.* Isolation, molecular characterization, and disinfectants susceptibility of swine-carried mammalian orthoreoviruses in Japan in 2020–2022. *J Vet Med Sci* **85(2)**, 185–193 (2023).

90. Intaruck K, Itakura Y, Kishimoto M, *et al.* Isolation and characterization of an orthoreovirus from Indonesian fruit bats. *Virology* **575**, 10–19 (2022).

91. Edgar RC. MUSCLE: multiple sequence alignment with high accuracy and high throughput. *Nucleic Acids Res* **32(5)**, 1792-7 (2004).

92. Letunic I, Bork P. Interactive Tree Of Life (iTOL) v5: an online tool for phylogenetic tree display and annotation. *Nucleic Acids Res* **49(W1)**, W293–W296 (2021).

93. Miller CL, Arnold MM, Broering TJ, *et al*. Localization of mammalian orthoreovirus proteins to cytoplasmic factory-like structures via non-overlapping regions of μNS. *J Virol* **84(2)**, 867–82 (2010).

94. Diller JR, Thoner TW, Ogden KM. Mammalian orthoreoviruses exhibit rare genotype variability in genome constellations. *Infect Genet Evol* **110**, 105421 (2023).

95. Murakami S, Kitamura T, Matsugo H, *et al*. Isolation of bat sarbecoviruses, Japan. *Emerg Infect Dis* **28(12)**, 2500-2503 (2022).

96. Jiang RD, Li B, Liu XL, *et al.* Bat mammalian orthoreoviruses cause severe pneumonia in mice. *Virology* **551**, 84–92 (2020).